Polymer 202 (2020) 122640

Contents lists available at ScienceDirect

Polymer

journal homepage: http://www.elsevier.com/locate/polymer

Poly(ionic liquid)s with engineered nanopores for energy and environmental applications

Huijuan Lin [a,1], Suyun Zhang [b,1], Jian-Ke Sun [c,**], Markus Antonietti [d], Jiayin Yuan [e,*]

[a] Key Laboratory of Flexible Electronics and Institute of Advanced Materials, Jiangsu National Synergetic Innovation Center for Advanced Materials, Nanjing Tech University, Nanjing, 211816, China
[b] Shenzhen Key Laboratory of Laser Engineering, Key Laboratory of Optoelectronic Devices and System of Ministry of Education and Guangdong Province, College of Optoelectronic Engineering, Shenzhen University, Shenzhen, 518060, China
[c] School of Chemistry and Chemical Engineering, Beijing Institute of Technology, Beijing, PR China
[d] Max Planck Institute of Colloids and Interfaces, Potsdam, 14476, Germany
[e] Department of Materials and Environmental Chemistry, Arrhenius Laboratory, Stockholm University, Stockholm, 10691, Sweden

ARTICLE INFO

Keywords:
Nanoporous PIL
Pore construction
Heteroatom-doped carbon
Energy storage and conversion
Environmental application

ABSTRACT

Poly(ionic liquid) (PIL) integrates some intrinsic characteristics of ionic liquids (ILs) with classic merits of polymeric materials, and opens up a new dimension to research ionic polymers. Nanoporous PILs with controlled nanopores combine the advantages of two classes of functional materials, *i.e.*, porous polymers and ILs, which greatly expand their applicability to energy storage and conversion, environmental sensing, gas sorption and catalysis. In this short review, we summarize the recent advances in the design and synthesis of nanoporous PILs, focusing on pore generation and engineering, electrostatic interactions, and potential applications to address energy and environmental issues. Porous carbons from nanoporous PIL templates/precursors are also briefly discussed as an extension of nanoporous PILs for energy research. Finally, our future perspectives on the potential of nanoporous PILs are presented.

1. Introduction

Porous polymers have received considerable attention in recent decades because of their broad applicability in energy storage and conversion, water purification, and sustainable development [1–3]. Functional materials derived from porous polymers in various forms, such as powders, membranes, sponges, and fibers, are used in industry and in daily life [4–6]. Ionic liquids (ILs), a class of molten salts with melting points below 100 °C, are formed by combinations of organic cations and organic or inorganic anions. They possess unique properties, such as negligible volatility, high ionic conductivity, good thermal/-chemical stability and tunable chemical structures [7]. Poly(ionic liquids) or polymerized ionic liquids, abbreviated "PILs", combine some of the intrinsic characteristics of both ILs and polymers and have the advantage of ion conduction, processability, durability and thermal stability; thus, they have attracted extensive interest in a broad range of potential applications [8–14]. PILs incorporate cations (*e.g.*, imidazolium, pyridinium, ammonium, phosphonium and guanidinium) and anions (*e.g.*, Cl^-, Br^-, I^-, BF_4^-, PF_6^-, $CF_3SO_3^-$ and $(CF_3SO_2)_2N^-$) common in IL chemistry into macromolecular architectures (Fig. 1). The second- and third-generation ILs developed starting in the 1990s notably contain halogen-free anions and biofriendly ions (*e.g.*, choline- or amino acid-based ions), and these ionic structures are missing or rarely involved in conventional ionic (anionic, cationic and zwitterionic) polymers. Thus, PILs research above all enlarges the structural toolbox to design innovative ionic polymers. PILs have the classic properties of ionic polymers, but they also have some of the unique properties of ILs, such as inflammability, relatively high ion conductivity, adaptive solubility, and possible low glass transition temperatures. The adaptive solubility of PILs, meaning the PILs are soluble in organic solvents over an unbelievably broad polarity range, such as chloroform, acetone and ethyl acetate, which usually cannot solubilize conventional ionic polymers, is quite notable. To be used widely and perhaps industrially, the cost of PIL production should be sufficiently low, ideally comparable to

* Corresponding author.
** Corresponding author.
E-mail addresses: jiankesun@bit.edu.cn (J.-K. Sun), jiayin.yuan@mmk.su.se (J. Yuan).
[1] These authors are equally contributed to this work.

https://doi.org/10.1016/j.polymer.2020.122640
Received 23 January 2020; Received in revised form 27 April 2020; Accepted 18 May 2020
Available online 23 May 2020

the current engineering plastics. The common methods of PIL synthesis currently in use involve monomer synthesis and sequential polymerization and are too costly. The newly emerging polyimidazolium synthesis *via* the Debus-Radziszewski reaction [15,16] skips the step of monomer synthesis and produces polyimidazolium derivatives directly from raw materials (diamine, diketone and aldehyde) in aqueous media at room temperature in a high yield (typically > 80%). This reaction might be a key breakthrough for low-cost PIL production. Within this polymer class, PIL networks with a nanoporous structure have emerged as especially promising [17–20]. Nanoporous PILs refer to PILs with pores smaller than 100 nm, which covers essentially all micro-, meso-, and macropores. To date, research has been focused on realizing precise control over the pore structure, morphology, chemical composition, and surface functionality. In addition, there is an interest in exploiting nanoporous PILs with high specific surface areas and finely tuned pore characteristics for applications where mass transport and the density of surface-active sites are important.

In comparison to well-developed neutral porous polymers [21–24], the incorporation of both small pores and charges into polymer networks has not been fully explored. The development of nanoporous PILs with ionic skeletons will greatly expand the application scope of porous polymers. In particular, nanoporous PILs possessing mobile counterions, which are absent in neutral systems, are promising for energy and environmental applications. Recent reviews on PILs have mainly focused on the synthesis of diverse molecular structures and their applications [17–20,25–27]. Here, we specifically highlight nanoporous PILs in terms of pore formation, tunable structure and materials applications.

2. Synthesis of nanoporous PILs

The porous architecture of nanoporous PILs determines their mass transport abilities and the number of active sites, which are closely related to their practical uses [27]. Generally, nanoporous PILs are synthesized by hard/soft template methods, electrostatic complexation, and postsynthesis modification, which are discussed below.

2.1. Template method

2.1.1. Hard template

The self-assembly of monodisperse colloidal particles has inspired templating processes to introduce systems with high porosity [28]. The hard template method is frequently adopted to prepare PIL membranes or thin films with well-ordered pore arrays [29–32], as this strategy facilitates precise control of the pore size and shape. When using colloidal crystals as hard templates, an opposite structure (an inverse opal) that replicates the periodicity of uniform colloidal particles over a large size scale is obtained. Li et al. [31] reported imidazolium-based PIL thin films with three-dimensional (3D) ordered macropores (Fig. 2a–c). The synthesis involved the preparation of monodisperse colloidal SiO_2 particles 260 nm in diameter, the polymerization of IL monomers in the SiO_2 template opal, and template removal. Specifically, the imidazolium-based IL was polymerized in situ in face-centered cubic (fcc) colloidal SiO_2 templates in the presence of a cross-linker and a thermal radical initiator, and the SiO_2 template was dissolved with HF solution. The resulting macroporous PIL membranes with an inverse opal structure could be employed as photonic crystal sensors and in electro-optic switching and molecular gating systems by simple counteranion exchange. However, the relatively low Brunauer-Emmett-Teller (BET) specific surface area (S_{BET} ~37 $m^2\ g^{-1}$) limits their suitability for applications in which a high S_{BET} is crucial, *e.g.,* in gas sorption, catalysis and batteries. By applying SiO_2 nanoparticles (NPs) 25 nm in diameter as templates, Wilke et al. [33] synthesized PILs with well-defined mesopores (Fig. 2d and e). The synthetic procedure was based on infiltration of an IL monomer/initiator mixture into opal-like silica templates (driven by capillary forces) formed by slowly drying an aqueous dispersion of silica NPs. Subsequent thermal polymerization of the IL monomer produced a transparent, amber-like silica-PIL hybrid. Here, the IL monomer itself was crosslinkable, giving the PIL a high cross-linking degree, which allowed the integrity of the mesoporous structure to be retained upon removal of the silica template by aqueous NaOH. The obtained mesoporous PIL reached a moderate S_{BET} of 200 $m^2\ g^{-1}$, making it more effective for CO_2 capture (~0.46 mmol g^{-1}) than nonporous PIL (~0.13 mmol g^{-1}). Such enhanced CO_2 uptake can be ascribed to the strong CO_2—PIL interactions as well as the enhancement in mass transfer due to the porous architecture.

The use of silica NPs (12 nm in diameter) as templates can also be extended to the preparation of nanoporous PILs by condensation polymerization *via* nucleophilic substitution between 1,3,5-tris(bromomethyl)benzene and 1,2-bis(4-pyridyl)ethylene [34]. The products possess hierarchical meso/macropores with S_{BET} values of 107–132 $m^2\ g^{-1}$ as well as a highly ionic skeleton that stabilized ultrasmall Au NPs (1–2 nm), delivering remarkable activity in the selective oxidation of saturated alcohols. Notably, the hard template method is not limited to silica but also to other inorganic materials, *e.g.*, $CaCO_3$ [35,36], TiO_2 [37] or Al_2O_3 [38].

2.1.2. Soft template

This method is based on the use of soft materials, primarily self-assembled block copolymers containing mesostructures in the bulk state, as soft-templates to direct the synthesis of porous materials [39]. Compared to hard templates, soft template methods largely rely on solvent extraction to remove the template after the formation of the crosslinked polymers either *via* chemical modification or direct polymerization of the IL monomers in the presence of a crosslinker inside the template. In the latter case, using a crosslinkable IL monomer is quite popular. In this regard, the polymerization is conducted in the presence of a soft template (*e.g.*, unreactive/inert soft polymers or porogenic solvents), followed by template removal after polymerization. Strong interactions between the template and the monomer are a prerequisite

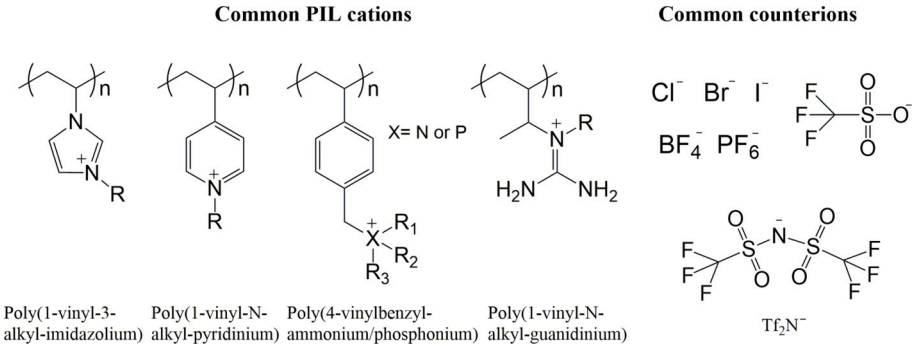

Fig. 1. Typical structures of PIL cations and their counterions.

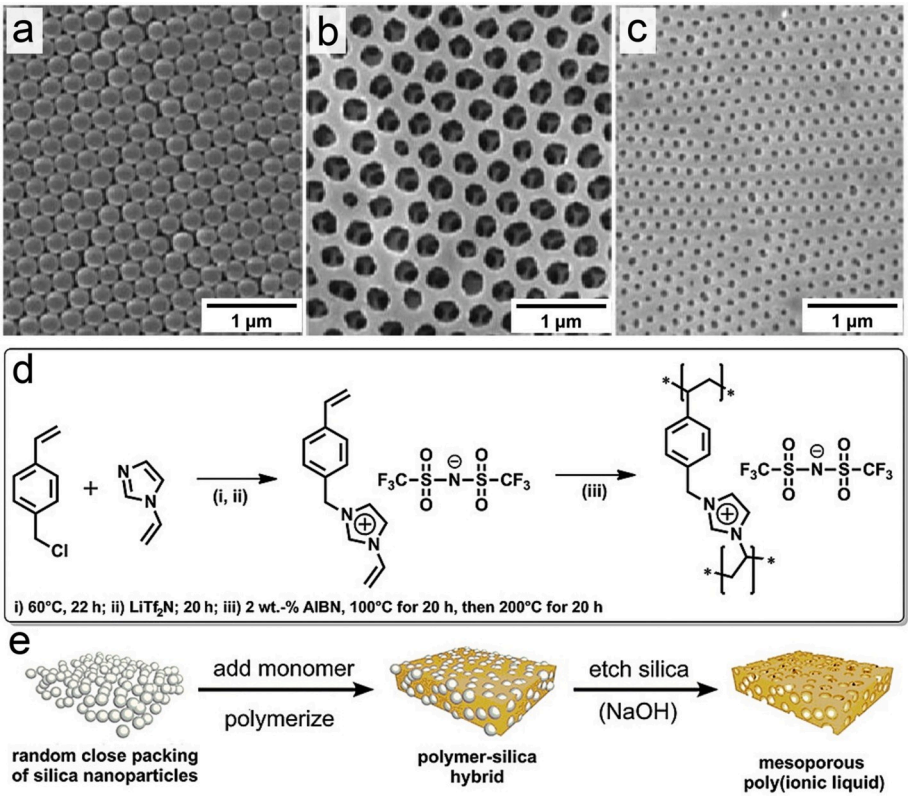

Fig. 2. SEM images of (a) the SiO_2 particle template, (b) well-ordered macroporous PIL with Br^- as the counteranion [poly(1-(2-acryloyloxyhexyl)-3-methylimidazolium bromide)], (c) and porous PIL after exchanging Br^- with Tf_2N^- [31]. Copyright 2010, Royal Society of Chemistry. (d–e) Synthesis of mesoporous PIL [poly(3-(4-vinylbenzyl)-1-vinylimidazolium bis(trifluoro methylsulfonyl)imide)] employing SiO_2 as a hard template [33]. Copyright 2012, American Chemical Society.

to replicate the template morphology and subsequent removal of template by solvent extraction, both of which influence the morphology of the resulting pores. When the soft template (porogen) can solvate the polymer chains well, it gives rise to small pores. Wang and coworkers [40] reported a hierarchically meso-/macroporous PIL with a tunable pore structure by utilizing a triblock copolymer, $EO_{20}PO_{70}EO_{20}$ (P123), as the template (Fig. 3). P123 was initially dissolved in water to form a micellar solution, and subsequently 1-allyl-3-vinylimidazolium IL monomer was added under vigorous stirring to fully dissolve the IL around the micelles. This was followed by polymerization in the presence of an initiator. The extraction of the micelle template by ethanol gave a porous PIL monolith. Importantly, the P123 and IL monomers had to be dissolved in water to ensure sufficient interaction and thermal equilibrium between the IL precursor and P123. According to the charge matching principle for synthesizing mesoporous materials with a template, P123 interacts with the IL cation in an acidic medium through a $S^0H^+X^-I^+$ mode (S^0: nonionic surfactant P123, H^+: hydrogen ions of ionization, X^-: IL anion, I^+: IL cation), which governs the assembly process and pore formation [39]. After removing the P123 template and subsequently introducing phosphotungstic anion $PW_{12}O_{40}^{3-}$ *via* anion exchange, the resulting mesoporous PIL can serve as an efficient heterogeneous catalyst for the epoxidation of *cis*-cyclooctene with H_2O_2 [40]. Odriozola and coworkers [41] explored nanoporous PILs by radical polymerization of bisvinyl-terminal ILs in the presence of non-polymerizable ILs as porogenic solvents. The pore size can be tuned in the range of 6.8–8.5 nm by varying the experimental parameters, such as the monomer/porogen ratio and the percentage of porogenic solvent.

Generally, due to the soft and organic nature of ionic polymeric networks, PILs prepared with the aforementioned methods, in the case of low and medium crosslinking densities, would undergo volume shrinkage and pore collapse after soft template or solvent removal. A strategy is needed to avoid or minimize structural shrinkage, maximize the retention of the organic porous matrix, and achieve textural engineering of PILs with stable and well-developed mesoporous frameworks. An example was illustrated recently by Xing and coworkers [42] who

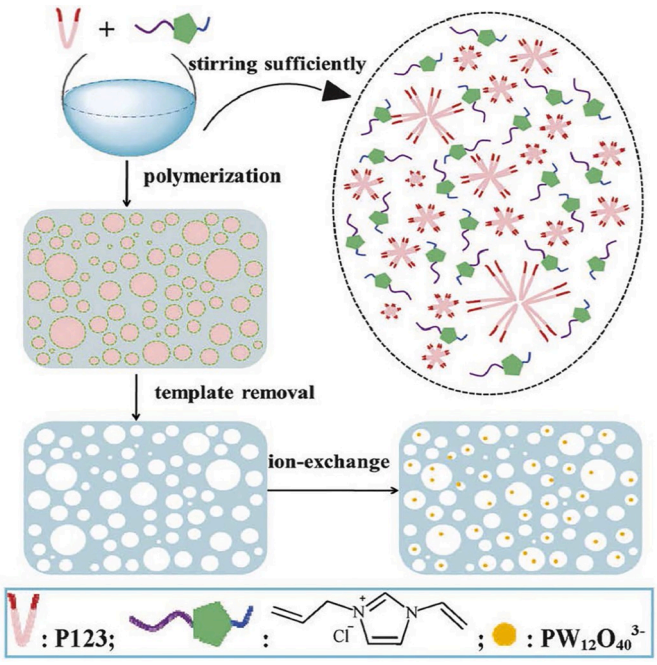

Fig. 3. Synthetic pathway to a hierarchically meso/macroporous PILs in the presence of a soft template P123 [40]. Copyright 2015, Royal Society of Chemistry.

used a hypercrosslinking approach to stabilize and rebuild collapsed labile mesoporous PIL networks and generate microporosity. The resultant nanoporous PIL with micro/mesopores exhibited enhanced performance in CO_2 capture (28.18 mg g^{-1} at 0 °C and 1 bar) and tocopherol absorption (211.45 mg g^{-1}).

2.2. Ionic complexation method

Porous PILs obtained *via* a templating method often possess a narrow pore size distribution, but the removal of the templates is often a labor-intensive, time-consuming procedure that can require hazardous etching reagents. Wang and coworkers reported a template-free route to obtain porous PILs *via* radical copolymerization of imidazolium-type ILs with divinylbenzene (DVB) as the cross-linker [43,44]. The porous structure can be easily tuned by the type of solvent, the alkyl chain length tethered to the imidazolium ring, or the molar ratio of IL monomer to DVB. Very recently, a template-free method based on ionic complexation was proposed as a cost-effective procedure. Our group applied this strategy to prepare micro/mesoporous PIL-PAA (poly(acrylic acid)) complex materials. Typically, hydrophobic PIL-Tf_2N (poly[1-cyanomethyl-3-vinylimidazolium bis(trifluoromethanesulfonyl)imide]) and PAA were homogeneously dissolved in dimethylformamide (DMF). In this solution, the PAA remained neutral, and no ionic complexation occurred between PIL and PAA. After dropping the above solution into 0.5 wt% NH_3-ethanol under sonication, a porous, yellowish, insoluble powder was obtained (Fig. 4a). During the ammonia treatment step, the carboxyl group in PAA was deprotonated to form the polyanion $PAA^-NH_4^+$, which ionically complexed with PIL. The complexed material had a mixture of micro/mesopores with an S_{BET} of ~310 $m^2\ g^{-1}$ [45].

The ionic complexation strategy was further exploited to fabricate hierarchically nanoporous PIL-PAA membranes with a gradient cross-linking along the membrane's cross-section (Fig. 4b). In this synthetic procedure, a homogenous mixture of PIL-Tf_2N and PAA was cast onto a glass slide and dried at 80 °C to evaporate the solvent (DMF). Then, the film was immersed in an aqueous NH_3 solution, during which ammonia diffused into the PIL-Tf_2N and PAA blend film to deprotonate PAA into the polyanion, affording $PAA^-NH_4^+$ and driving the electrostatic complexation between PIL-Tf_2N and the in situ generated $PAA^-NH_4^+$. Simultaneously, due to the hydrophobic fraction of PIL-Tf_2N in the blend film, phase separation occurred upon diffusion of water into the film, which created interconnected nanopores ranging from 30 to 100 nm [46]. Notably, this method can be extended to hydrophilic PILs (*e.g.*, imidazolium PIL with a hydrophilic anion such as Br^-) [48], with different molecular weights (M_w) of PAA [49] or even multivalent carboxylic acids instead of polyacids [47]. For example, by employing multivalent benzoic acid derivatives instead of PAA, a PIL-based membrane with tailored pore sizes in the range of 80 nm to 2.5 μm could be made (Fig. 4c–f) [47]. The abovementioned electrostatic cross-linking strategy is facile, efficient and scalable, and most importantly, it does not require an external template. This strategy was recently shown to be compatible with other nanofabrication techniques, such as 3D printing, as exemplified by hierarchically porous 3D-printed patterns featuring exceptional sensing properties [50]. When introducing a dicyanamide anion (DCA) to replace Tf_2N^-, additional covalent cross-linking to form an *s*-triazine network could be initiated by thermal annealing of the nanoporous membrane, which further stabilized the porous structure in a solution of high ionic strength and afforded a material that can be used in applications requiring harsh conditions [51].

2.3. Postsynthetic modification

Unlike direct synthesis strategies with or without a template, nanoporous PIL can also be achieved by postsynthetic modification of neutral porous polymeric networks, typically through quaternization reactions. For instance, Liu et al. [52] obtained mesoporous PILs with pore sizes ranging from 10 to 40 nm by quaternization and follow-up anion exchange (Fig. 5). In detail, divinylbenzene (DVB) and 1-vinylimidazole (vim) were first copolymerized at 100 °C under solvothermal conditions in ethyl acetate to afford a neutral, crosslinked mesoporous polymer (PDVB-vim). After quaternization of PDVB-vim with CH_3I, the I^- anion was exchanged with $SO_3CF_3^-$ to afford PDVB-[C1vim][SO_3CF_3], which exhibited a higher base-catalytic activity than the soluble monomer [C1vim][SO_3CF_3] in several test reactions, including transesterification, Peckmann reaction, Kharasch addition, and hydration, due to better wettability with the reactants (*e.g.*, tripalmitin and methanol). Although this strategy is versatile and can afford nanoporous PILs that are difficult to synthesize *via* direct ionic network synthesis, such an approach usually decreases the surface area and porosity. For example, the surface area was found to be reduced from 670 (PDVB–vim) to 181 $m^2\ g^{-1}$ (PDVB-[C1vim][SO_3CF_3]). Therefore, care should be taken to maintain the surface area and pore structure after ionization of the pores. One possible solution to this issue is to judiciously select porous polymer templates with high surface areas and chemical stability as starting materials. In this regard, sufficient surface area can be retained

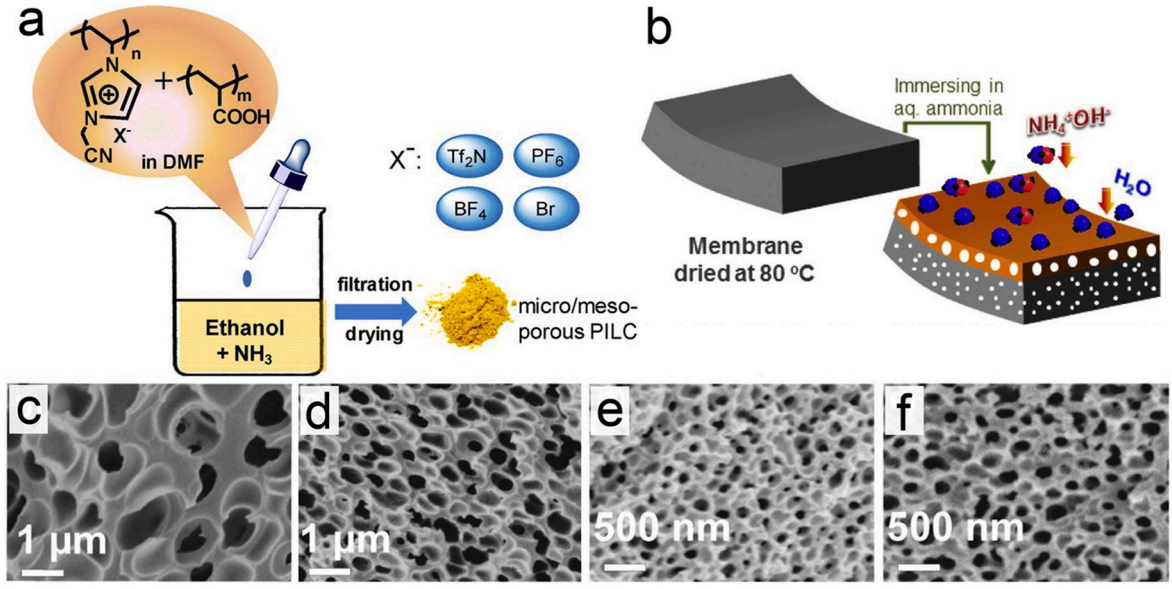

Fig. 4. (a) The preparation of a micro/mesoporous PIL-PAA complex powder (PIL-Tf_2N and PAA) *via* electrostatic complexation [45]. Copyright 2012, American Chemical Society. (b) Illustration of pore formation in the PIL-PAA complex membrane after NH_3 treatment [46]. Copyright 2013, American Chemical Society. (c–f) Cross-sectional SEM images of membranes prepared from PIL-Tf_2N and benzoic acid bearing 2, 3, 4, or 5 carboxylate groups, respectively [47]. Copyright 2015, American Chemical Society.

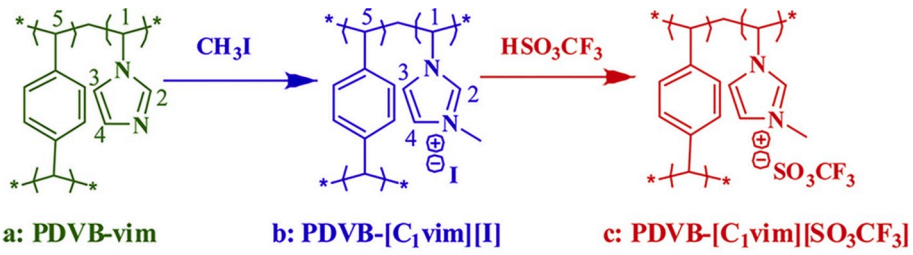

Fig. 5. The synthetic scheme for the preparation of PDVB-[C1vim][SO_3CF_3] from PDVB-vim [52]. Copyright 2012, American Chemical Society.

after the introduction of functional moieties onto the pore walls. An example was revealed by Wu and workers, who functionalized polymer materials with well-ordered mesopores (FDU-14, S_{BET}: 545 m^2 g^{-1}, FDU-15, S_{BET}: 463 m^2 g^{-1}) with –SO_3H. The porosity of the post-synthetically altered materials was well maintained without obvious damage (FDU-14–SO_3H, S_{BET}: 539 m^2 g^{-1}, FDU-15–SO_3H, S_{BET}: 447 m^2 g^{-1}) [53].

Generally, anions preferentially occupy interstitial voids during the polymerization of ionic monomers. In principle, when the bulky anions of PILs are exchanged for smaller anions, a portion of the occupied space can be recovered to regenerate pores. Recently, Gao et al. [54] employed such a strategy to synthesize hierarchically porous PILs. The copolymer PIL obtained by direct copolymerization of 1,4-butanediyl-3,3′-bis-1--vinylimidazolium disalicylate (BVImSal) and DVB was poorly porous (S_{BET}: 15.1 m^2 g^{-1}). After exchange of the salicylate ions with NaX (X = Cl, Br and OAc), the resulting PILs possessed hierarchical micro/-mesopores with enhanced surface areas (PIL-Cl: 227.5 m^2 g^{-1}, PIL-Br: 180.6 m^2 g^{-1}, PIL-OAc: 129.2 m^2 g^{-1}). Moreover, the smaller anions (Cl^-, Br^- and OAc^-) of the porous PILs resulted in a higher specific surface area.

2.4. Other methods

Several other methods for preparing nanoporous PILs have been reported. Texter and coworkers synthesized copolymer gels by polymerization of microemulsions stabilized by a polymerizable IL surfactant [55,56]. The copolymer structures can be transformed between hydrogel and porous structures by anion exchange of the IL moiety of the copolymer. By exchanging BF_4^- for PF_6^-, the copolymers changed from a hydrophilic (hydrogel) to hydrophobic state, thus shrinking the polymer domains at the interface to form pores in water. Furthermore, the porous polymer can be reversibly converted into a swollen gel when transferred from an organic solvent (*e.g.*, dimethyl sulfoxide (DMSO) or DMF) to water [55]. The striking gel/pore switching makes this a promising functional porous PIL for controlled release in drug delivery applications.

Recently, Schlenoff and coworkers presented the concept of “saloplastic” PIL complexes, which are ionically cross-linked materials comprising polycations and polyanions, *e.g.*, poly(styrenesulfonate sodium salt) (PSS) and poly(diallyldimethylammonium chloride) (PDADMA), that can be reshaped by breaking sufficient cross-link points using concentrated salt solutions [57,58]. Interestingly, these materials can also be processed into a porous state with tunable mechanical properties by varying the salt (ionic strength), demonstrating the promising applicability of saloplastic complexes for bioimplants.

3. Nanoporous PILs for energy applications

Porous PILs have great potential for applications in energy storage devices. Their charged nanoporous structures and polymer backbones facilitate ion conduction and result in wide potential windows, making them suitable as electrolytes and separators for battery applications. In addition, porous carbons from the pyrolysis of nanoporous PILs display appealing features such as rich heteroatom doping, tunable surface areas, and sufficient active sites for electrochemical processes.

3.1. Battery electrolyte

Considering the outstanding features of PILs, including their high thermal stability, wide electrochemical window, and high ionic conductivity, solid polymer electrolytes applying PILs in combination with an IL and a lithium salt as the hosts are promising alternatives to liquid electrolytes to avoid leakage issues [59–62] for high-safety batteries. However, the popular hybrid electrolytes of Li salt ($LiTf_2N$) and guanidinium-based PIL (1.17×10^{-4} S cm^{-1} at 80 °C) [59], trimethylammonium-based PIL (7.58×10^{-4} S cm^{-1} at 60 °C) [63], imidazolium-based PIL (1.89×10^{-5} S cm^{-1} at 25 °C) [64], and dicationic PILs (4.6×10^{-5} S cm^{-1} at 25 °C) [65] possess relatively low ionic conductivities (~10^{-5} S cm^{-1} at 25 °C) compared with organic liquid electrolytes in LIBs (~10^{-2} S cm^{-1} at 25 °C).

To enhance their ionic conductivity, Zhou et al. reported a hierarchical PIL-based solid electrolyte (HPILSE) to satisfy the required ionic conductivity as well as the mechanical strength for high-safety Li-/Na-ion batteries. This HPILSE film was prepared *via* the in situ polymerization of 1,4-bis[3-(2-acryloyloxyethyl)imidazolium-1-yl]butane bis[bis(trifluoromethanesulfonyl)imide] (C1-4TFSI) monomer with the 1-ethyl-3-methylimidazolium bis(trifluoromethanesulfonyl)imide (EMITFSI)-based electrolyte in the pores of a poly(diallyldimethylammonium bis(trifluoromethanesulfonyl)imide) (PDDATFSI) porous membrane (Fig. 6) [66]. The porous PDDATFSI membrane and the EMITFSI-based electrolyte at a suitable concentration provided good mechanical strength (2.4 MPa) and high ionic conductivity (>10^{-3} S cm^{-1} at 25 °C), respectively. In addition, the crosslinked poly(C1-4TFSI) framework in a quasi-solid state avoided the leaching of the EMITFSI-based electrolyte even at high temperature. Such distinctive integration properties offer great potential, as polymer electrolytes can reduce resistance and polarization for batteries with high performance. When using HPILSE for Li-/Na-ion battery applications, the in situ synthesis strategy ensures sufficient interfacial contact between HPILSE and the electrodes to lower the interfacial resistance (including the solid electrolyte interface (SEI) resistance (R_{SEI}) and the charge transfer resistance (R_{ct})) and buffer volumetric changes of the electrodes during the charge-discharge process, thus exhibiting electrochemical performances superior to those of polymer batteries of $LiFePO_4$/HPILSE/Li (81.4 mAh g^{-1} at a current rate of 1C, a capacity retention of 97.7% after 100 cycles at 0.1C) and $Na_{0.9}[Cu_{0.22}Fe_{0.30}Mn_{0.48}]O_2$/HPILSE/Na (59.9 mAh g^{-1} at 1C, a capacity retention of 85.5% after 100 cycles at 0.1C). This design balances the ionic conductivity and mechanical properties, presenting porous PIL-based materials that are promising solid electrolytes for next-generation batteries with satisfactory performance and safety.

3.2. Battery separator

Vanadium flow batteries (VFBs) are emerging as promising large-scale energy storage devices due to their attractive features of high safety, good energy efficiency and long-term stability [67–71]. Ideal VFB membranes are designed with the combined advantages of excellent proton conductivity, low vanadium ion permeability and high

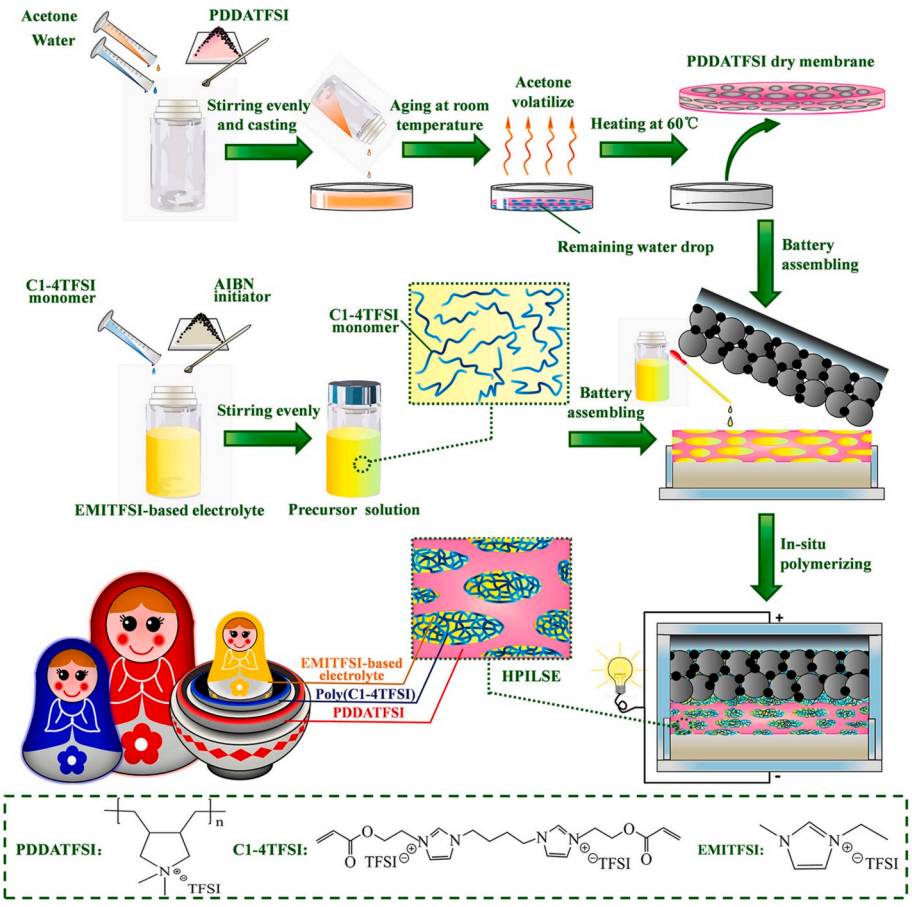

Fig. 6. Schematic of the synthesis of a nesting doll-like hierarchical PIL-based solid electrolyte (HPILSE) [66]. Copyright 2017, Elsevier.

mechanical and chemical stability [72–74]. An efficient approach to improve the V/H selectivity of VFB membranes is to introduce positively charged groups into the porous membrane on the basis of pore size exclusion and Donnan exclusion mechanisms, which can explain the exclusion of larger, higher valent vanadium ions while protons travel relatively freely. Following protonation of the N atoms of pyridine (Py) or imidazolium under acidic conditions, the membranes showed facile proton transport [75,76]. Zhang et al. designed a type of porous charged membrane with a symmetric spongy structure [75]. First, sponge-like chloromethylated polysulfone (CPSF) membranes were prepared *via* a

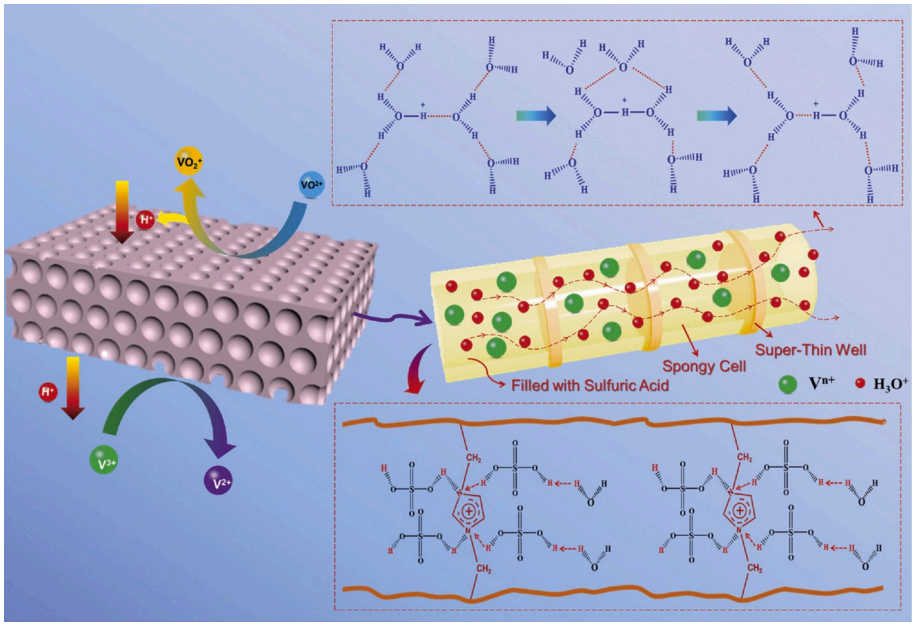

Fig. 7. Principle of a positively charged membrane in a sponge structure and internal crosslinking networks for VFB applications [76]. Copyright 2016, Wiley.

vapor-induced phase inversion method, comprising a large number of micron-sized cells. By grafting weak alkaline groups, *e.g.,* Py, onto the CPSF resin *via* nucleophilic substitution, the resulting CPSF-Py membrane was equipped with positive charges. The positive charges and disconnected pores offer enhanced ion selectivity. In addition, the grafted weakly alkaline groups can also bind the sulfuric acid that fills the membrane pores to ensure proton conductivity, thus facilitating proton transport. When applied for VFB, the resultant membrane realized an energy conversion efficiency (EE) of over 88% under 40 mA cm^{-2} and over 81% under 120 mA cm^{-2}, outperforming Nafion 115 membranes. To further improve the membrane stability for practical applications, further studies were conducted by the same group by constructing internal crosslinking networks on the pore walls of the CPSF membranes (Fig. 7) [76]. Specifically, a positively charged imidazole group (imidazolium) was reacted with CPSF to form an internal crosslinking network on the pore walls. The CPSF membrane with a cross-linking time of 72 h in the imidazole solution (denoted CPSF-72) exhibited a columbic efficiency (CE) above 99% and an EE of 86% at a current density of 80 mA cm^{-2}, much higher than that of Nafion 115, suggesting a high ion selectivity attributable to pore size exclusion and Donnan exclusion effects from the positively charged imidazolium groups. In addition, a VFB single cell assembled with CPSF-72 delivered a stable performance over 6000 cycles at 120 mA cm^{-2} as well as a nearly unchanged membrane morphology after cycling, indicative of the excellent stability of the membrane.

3.3. Nanoporous PIL-templated carbon materials for energy applications

Porous carbon materials are attractive and versatile platforms with applications in environmental remediation and energy storage and conversion. Among the wide variety of carbon precursors available, PILs, with their myriad structures and compositions, offer enormous advantages for the synthesis of heteroatom-doped porous carbon materials. The introduction of heteroatoms (*e.g.*, nitrogen, boron, and phosphorus) into the graphitic carbon network could vary their bulk or surface state to tune their optoelectronic properties and/or chemical activities, which are useful particularly for energy conversion and storage. Three factors are of importance in determining the properties of porous carbon materials, *i.e.,* the morphology, porosity and atomic structure. The organic solution processability of PILs allows access to diverse morphologies that may be difficult to achieve using traditional polyelectrolytes. Employing appropriate pyrolysis techniques, *e.g.,* vacuum carbonization, the morphology of the PIL could be well maintained in the final product, which could provide carbon materials with multifarious porous structures and thereby optimize their functions. As ILs are composed of cation and anion pairs, the structures and properties of PILs can be finely tuned by either tethered cations or anions. Therefore, the judicious selection of PIL constituents can be used to control the porosity of the resulting porous carbons, offering a straightforward way to prepare porous carbon materials by carbonization of the polymer precursor. The structural advantage PILs, which often control the atomic structure of the carbon material, is the presence of heteroatoms in their structures. These heteroatoms could be readily incorporated into the carbon framework during carbonization, which in turn alters the physicochemical properties of the carbon material and results in unusual properties.

In 2009, Antonietti et al. opened up this field by using an imidazolium PIL as a precursor to produce mesoporous carbon nanostructures in the presence of $FeCl_2$ [77]. Here, PIL acted as the carbon precursor with a metal salt ($FeCl_2$) as the catalyst to control the morphology of the obtained carbon nanosheets. During carbonization, Fe^{2+} was reduced to iron and iron carbide NPs, dissolving amorphous carbon into the iron particles and subsequently precipitating graphitic carbon following a so-called dissolution/precipitation mechanism. Pure carbon nanomaterials with mesoporous and graphitic structures were obtained after acid etching, and the materials showed a high surface area and low electric resistance [78]. Instead of using a nonporous PIL as the carbon source, the direct carbonization of a mesoporous PIL with $[Fe(CN)_6]^{3-}$ anions generated porous carbon particles. The unique mesoporous ionic networks enabled the molecular dispersion of ferric precursors and therefore resulted in highly dispersed Fe_2O_3 NPs on the carbon material, and it showed remarkable catalytic performance in the oxidation of benzene to phenol [79].

Dai and coworkers employed a nanoporous PIL as a template and precursor for nitrogen-doped porous carbon materials [80–82]. As a typical example, nitrogen-doped porous carbon materials were obtained *via* the direct pyrolysis (trimerization and carbonization) of IL precursors bearing cations with nitrile groups, which could form stable triazine rings *via* a thermal condensation reaction (Fig. 8). The formation of carbon materials proceeded *via* the cross-linking of the monomeric IL precursor, resulting in dynamic/reversible porous polytriazine networks through cyclotrimerization between three nitrile groups (at < 400 °C) with a large amount of paired anion remaining. An irreversible carbonization reaction involving the formation of a C–C bond with concomitant H_2 release occurred at elevated temperatures (>400 °C). Notably, the porous architecture of the obtained carbon materials from further carbonization at 800 °C is strongly dependent on the cation/anion structures within the ILs. For example, carbon materials derived from 1-cyanomethyl-3-methylimidazolium ($[MCNIm]^+$) with Tf_2N^- (MCNIm-Tf_2N) featured dominant mesopores, whereas only micropores were found for carbon materials from 1,3-bis(cyanomethyl) imidazolium ($[BCNIm]^+$) with Tf_2N^- (BCNIM-Tf_2N). In addition, the anion structure also impacts the porosity of the resulting material. Carbon materials derived from [BCNIm][Tf_2N] and [BCNIm][beti] had higher surface areas, whereas materials from the same cation with Cl^- were almost nonporous, demonstrating the templating or catalytic role of bulky anions during pore generation.

Recently, nanoporous PILTf_2N-PAA membranes were pyrolyzed under vacuum to produce nitrogen-doped carbon membranes with hierarchical porous structures [84]. According to thermogravimetric analysis, these polymer membranes first underwent trimerization of the cyano groups to build a stable triazine network [85]. The formed porous network is controlled by the M_w of PAA, *i.e.*, a higher M_w of PAA results in a higher cross-linking density, thus giving smaller pores. The synthetic route was facile, straightforward and scalable and produced a macroscopic membrane, here 10.5 × 3.5 cm^2. The resulting carbon membranes featured hierarchical porous structures, high nitrogen doping and high electric conductivity, which resulted in high surface areas and rapid mass diffusion suitable for electrochemical applications. For example, after hybridization with carbon nanotubes, nitrogen-doped carbon/CNT membranes showed appealing performance in the electrocatalytic conversion of CO_2 to formate with a high Faradaic efficiency of 81% [86]. Furthermore, by loading Janus-type Co/CoP NPs [87], these hybrid membranes can be used as active electrocatalysts for hydrogen evolution reactions in both acidic and alkaline conditions, exhibiting great potential for practical applications.

4. Nanoporous PILs for environmental applications

The distinctive structural features associated with the pores and charges in nanoporous PILs make them suitable for gas uptake, sensing, separation, *etc*. For example, porous PILs can be engineered into environmental sensors/actuators in response to humidity, temperature, pH, etc. *via* the rational design of the functional sites. Due to the high surface area and charged properties offered by porous PILs, they can be further processed into nanoporous membranes for heavy metal ion [88] and organic pollutant absorption [89].

4.1. CO_2 capture

The efficient capture of CO_2 is attracting widespread interest for mitigating greenhouse gas emissions. It was demonstrated that PILs have

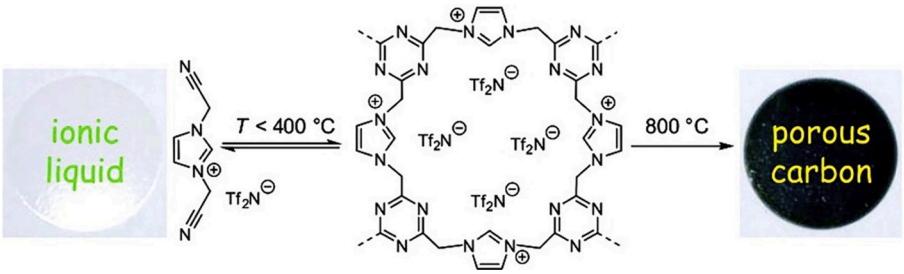

Fig. 8. The carbonization of an IL with nitrile groups to obtain a nitrogen-rich porous carbon material [83]. Copyright 2009, American Chemical Society.

higher CO_2 sorption capacities with faster sorption/desorption rates than their corresponding monomeric ILs under similar conditions [90,91]. Introducing porosity into PILs can amplify their CO_2 capture abilities due to the larger volume of accessible space compared with their nonporous counterparts. In addition, ionic pore walls contribute to the build-up of Coulombic fields required for polarization and the polarized binding of polar molecules. A mesoporous PIL was investigated at 273 K and 1 atm of CO_2, and it exhibited a CO_2 uptake of 0.46 mmol g^{-1}, higher than those of the IL monomer (0.02 mmol g^{-1}) and bulk PIL (0.13 mmol g^{-1}) [33]. To optimize the CO_2 sorption capacity to a PIL, specific attention needs to be paid to the PIL architecture, including the polymer backbone, porosity, and counterions. Shen et al. studied the CO_2 absorption behavior of PILs with various structures, including different cations, anions, backbones, and substituents. The molecular structure of the PIL impacts its CO_2 sorption behavior. Its CO_2 sorption capacity is greatly influenced by the type of cations, and the capacities are in the order tetraalkyl ammonium > pyridinium > phosphonium > imidazolium cations. Tetraalkyl ammonium-type PILs interact more strongly with CO_2, and this can be attributed to the high positive charge density on the tetraalkylammonium cations. Furthermore, the CO_2 capture capacities of PILs with different anions follow the order BF_4^- > PF_6^- > Tf_2N^-. However, PILs with longer alkyl substituents on the cation showed decreased CO_2 uptake, probably due to steric hindrance and weakened CO_2–cation interactions. Moreover, the CO_2 sorption isotherm can be well fitted by a dual-mode model, suggesting that CO_2 sorption consists of dissolution in the polymer matrix and Langmuir sorption in the pores [92].

It should be mentioned that imidazolium-type cationic polymers preferentially form imidazolium–carboxylates formally *via* a transient *N*-heterocyclic carbene (NHC) intermediate for CO_2 capture. In this process, CO_2 is chemically converted into zwitterionic adducts at room temperature, and the fixed CO_2 can be released at elevated temperature [93]. Taton and coworkers [94] reported an imidazolium-based PIL, which was treated with a strong base (potassium butoxide) to deprotonate the C2 position of the imidazolium ring to produce poly(*N*-heterocyclic carbene) (denoted poly(NHC)). This poly(NHC) further reacted with CO_2, forming poly(NHC–CO_2) adducts with carboxylate species appended to the imidazolium ring. The thermally unstable imidazolium carboxylate zwitterion underwent decomposition upon heating, accompanied by the release of CO_2, thereby stimulating the reversible adsorption/desorption process (Fig. 9). The combination of physical and chemical absorption was further demonstrated in a recent report on mesoporous imidazolium-type PIL-based polyampholytes. It was found that in addition to fast CO_2 adsorption on the surface of the ionic network (which is the predominant mechanism in typical micro/mesoporous organic polymers), volume uptake and swelling deep into the polymeric matrix also occurred. This process was slow compared to surface adsorption and came with an energetic penalty, which was attributed to the formation of an NHC intermediate within low-molecular-weight imidazolium-carboxylic anion-type ILs [95].

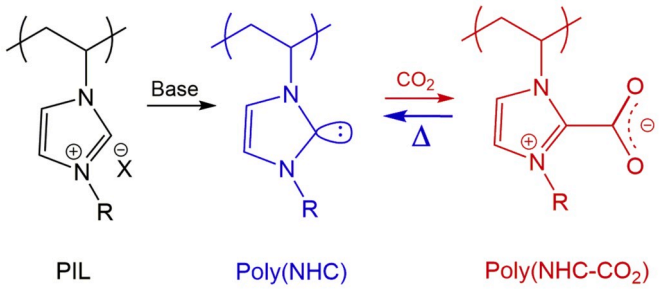

Fig. 9. The reaction of PILs containing an *N*-heterocyclic carbene (NHC) with CO_2 [94]. Copyright 2011, American Chemical Society.

4.2. Heterogeneous catalysis

Nanoporous PILs with charge-decorated pore surfaces and intrinsic porosity present new opportunities for heterogeneous catalysts. The charged pore can stabilize and support both metal ions and metal nanoparticles (MNPs), while the intrinsic ionic units on the pore walls can be used as functional sites for catalytic applications. Zhao et al. [45] reported a porous imidazolium-type PIL-PAA complex with a moderate specific surface area (330 m^2 g^{-1}) and charged pores for loading a metal salt ($CuCl_2$), and this material efficiently catalyzed the aerobic oxidation of C–H bonds. In addition to the abovementioned advantages, the charges on the nanoporous network endow additional functionalities, such as polarity and selective accessibility, which are beneficial for selective catalysis [96]. Wang and coworkers [97] used mesoporous PIL copolymers as supports to immobilize palladium (Pd) NPs that can efficiently and selectively oxidize benzyl alcohol to benzaldehyde with O_2 as the oxidant and water as the solvent. The small Pd NPs, as well as the amphipathic organic mesopore surface, accounted for the excellent performance. The synergy between PILs and MNPs was further demonstrated by a binary catalyst composed of an acid and a redox unit for the direct synthesis of 2,5-diformylfuran (DFF) from fructose. The nanoporous PIL functionalized with carboxylate groups after the loading nanobelt α-CuV_2O_6 served as a binary catalyst, giving a 63.1% yield of DFF in the one-pot and one-step conversion of fructose to DFF under atmospheric O_2 (135 °C, 3.5 h) [98]. The hydrophilic surface of the PIL enabled the preferential adsorption of fructose on the acid sites, whereas α-CuV_2O_6 showed strong adsorption of HMF but weak affinity for fructose. Such surface wettability-controlled adsorption inhibited the oxidation of fructose and facilitated the transfer of HMF to the oxidative sites on active α-CuV_2O_6.

Porous PILs carrying a high ion density and a large surface area have been applied for CO_2 absorption and conversion. The ionic surfaces offer strong CO_2 affinities through dipole−quadrupole interactions, thus enhancing CO_2 sorption and fixation, and the counteranions can act as active sites to facilitate the catalytic conversion of CO_2 [12,101,102]. Wang et al. reported a hierarchically meso/macroporous PIL ionothermally synthesized through the free radical polymerization of a bis-vinylimidazolium salt monomer (Fig. 10a) [99]. The as-synthesized

porous PIL catalyst exhibited excellent catalytic activity in the heterogeneous cycloaddition of CO_2 to cyclic carbonates, giving high yields (up to 90%) at low temperature (down to 70 °C) under solvent-free conditions over a wide range of substrates, including relatively inert epoxides with long alkyl chains. The improved performance can be explained by the mechanism considering two factors: (a) the well-dispersed active sites (Br^-) and the accelerated mass transfer of the substrates/products and (b) the intrinsic CO_2-philicity attributed to the enrichment of Br^-, which increased the CO_2 concentration at the active sites in the PIL framework. Furthermore, the same group reported a nanoporous PIL functionalized with $–NH_2$ [100] as a catalyst for the cycloaddition of CO_2 over various substrates under ambient pressure at < 100 °C (Fig. 10b). A mechanistic investigation revealed a possible reaction route through which the PIL bearing an amino-functionalized IL unit and the basic OH^- counteranion directly react with CO_2 to form HCO_3^-/NHCOOH intermediates in situ during the ring opening process, showing better CO_2 affinity than conventional Lewis bases, *e.g.,* Br^-, thus promoting the nucleophilic ring opening reaction.

4.3. Environmental sensing and actuation

Nanoporous PILs have been recognized as excellent candidates for sensing applications. A decorated PIL pore wall can initiate a variety of interactions (ionic, covalent, and noncovalent) between the IL species in the PIL and external chemical stimuli (solvents, ions, gas, radicals, etc.). Moreover, nanoporous materials have advantages such as low densities, large surface areas, and fast transport/diffusion, which can enhance their sensing performance. In the past few years, nanoporous PILs have been designed as sensors and actuators in response to external stimuli (humidity [29,103], pH [46], ions/gases [30,104,105], temperature [106], potential [107], etc.).

A nanoporous PIL-PAA membrane with nanopores 30–100 nm in size was prepared by a simple solution casting and NH_3-activation procedure. When coating this membrane on an optical fiber, it demonstrated superior pH sensing speed (t_r = 5 s, t_f = 12 s) and sensitivity (2.04 and −2.48 nm/pH unit) due to its highly charged and nanoporous nature [46]. More recently, such ionic complexed membranes were further processed into micropatterns *via* a photolithography approach. Being simultaneously microstructured and porous, the PIL micropatterns loaded with Pt NPs were readily engineered onto an electrode and served as a sensor for detecting H_2O_2 down to 45 mM [50].

Li et al. found that porous PIL films can be converted into functional films for ion detection and molecular recognition [29–32,108]. These films were fabricated from a hard template approach and carried 3D ordered macropores. Imidazolium-based ILs with different anions (hydrophilic or hydrophobic) can have different solubilities. When combining the distinct properties of ILs and photonic crystals, volumetric changes can be induced by changing the solvent to give rise to the stop-band shift of the photonic PIL films with different anions through an exchange process in solution. For instance, a photonic PIL film in a 3D-ordered inverse opal structure obtained on a PMMA substrate could detect anions (Fig. 11). This platform provides a simple strategy for visual ion sensing with the naked eye. Furthermore, the same group combined this photonic structured PIL with a luminogen showing aggregation-induced emission (AIE) to develop a highly integrated sensing platform for saccharides [109]. Due to the integration of the

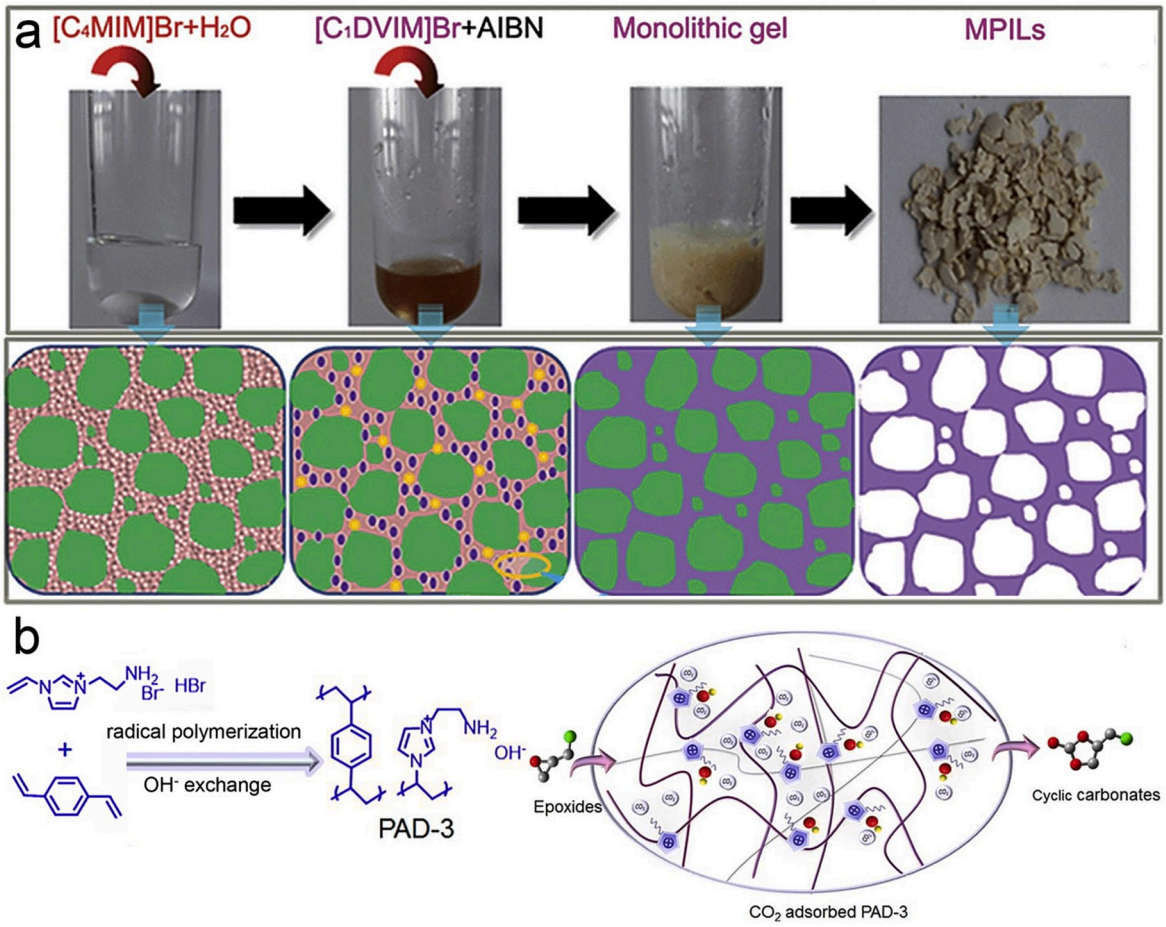

Fig. 10. (a) Photographs of a mesoporous PIL prepared *via* ionothermal synthesis [99]. Copyright 2015, Royal Society of Chemistry. (b) Schematic of the preparation of a mesoporous PIL (PAD-3) for CO_2 adsorption and cycloaddition [100]. Copyright 2016, American Chemical Society.

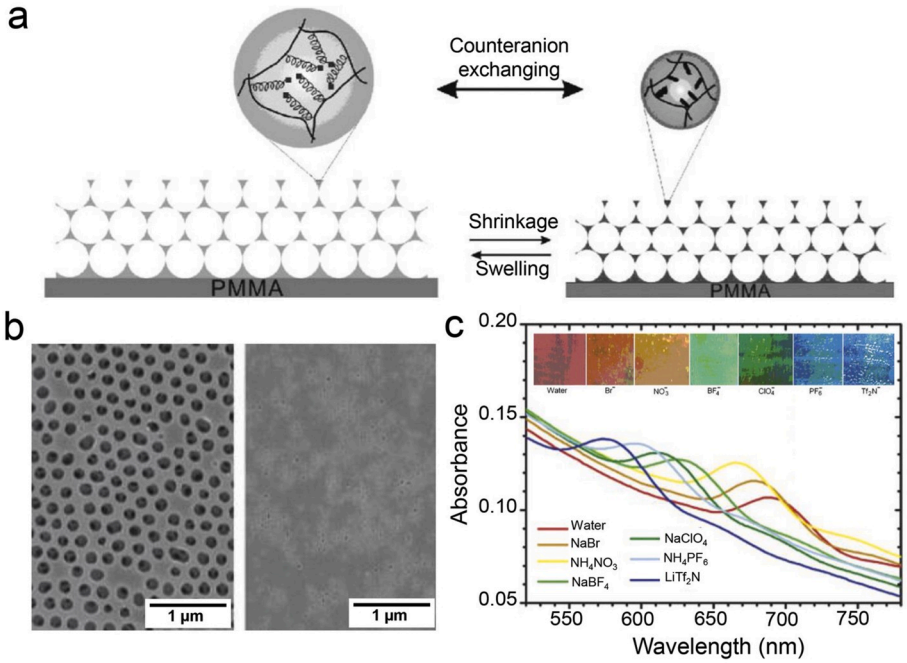

Fig. 11. (a) Schematic of the volume change of a porous photonic PIL film with different anions. (b) SEM images of the photonic PIL film with opened (left) and closed (right) pore structures. (c) Optical response of a porous photonic PIL film upon exposure to different anions [30]. Copyright 2008, Wiley.

binding effects between PILs and saccharides, which involve multiple noncovalent interactions, such as dominant hydrogen bonding, electrostatic forces and π–π interactions, the doped photonic structured PIL spheres showing AIE can discriminate numerous saccharides and show obvious color changes and altered fluorescence intensities. In particular, an imidazolium-type PIL sphere achieved a higher classification accuracy (100%) than ammonium (71%) or phosphonium cations (83%) toward 13 saccharides at a concentration of 10 mM. This outstanding performance can be explained by the stronger acidity of C2–H in the imidazolium cation ring, which is beneficial for forming hydrogen bonds with saccharides. The utilization of one PIL sphere to construct an integrated sensing platform offers a new way to identify saccharides with enhanced efficiency with a simple sensing system.

Increasing interest has been paid to exploring polymeric actuators for sensing organic solvents. In principle, the actuating performance of a nanoporous PIL membrane relies on its porous structure to accelerate mass transport while lowering the bending rigidity, thus accelerating the bending motion. Zhao et al. constructed a nanoporous actuator prepared by the in situ ionic complexation of a hydrophobic PIL-Tf_2N and a C-pillar[5]arene, featuring a gradient crosslinking density along the membrane cross-section [110]. The resultant PIL membrane actuator showed an ultrafast response toward acetone vapor (24 kPa, 20 °C), which could be explained by the inhomogeneous swelling resulting from the gradient of electrostatic complexation along the membrane cross-section and strong PIL-acetone interactions. In addition, in combination with its porous structure, the nanoporous PIL membrane exhibited a fast bending speed due to the accelerated diffusion of the acetone molecules into the membrane. When C-pillar[5]arene was replaced by PAA, the porous PIL-Tf_2N-PAA membrane could readily bend in water upon the addition of acetone, reaching a bending curvature (the reciprocal of the radius of the bent membrane) of 0.076 mm^{-1} triggered by a low concentration of acetone in water (0.25 mol%) (Fig. 12a and b), which was at least one order of magnitude more sensitive than the state-of-the-art solvent-responsive polymer gel actuators at the time of its publication [49]. By carefully controlling the pore size inside the PIL membrane and the polymer-solvent interactions, several types of organic solvents, even two butanol isomers, could be detected and distinguished (Fig. 12c).

In another design, a hydrophilic porous membrane was fabricated from a vinylimidazolium-based PIL, and pore variations (open and close states) were observed in isopropanol and water due to pore swelling [48]. By introducing structural complexity and functionality into the ionic complexed membrane, a tandem-gradient nanoporous membrane actuator based on polytriazolium-trimesic acid (ptraiz-TA) was obtained, which carried two structurally independent gradients, in the electrostatic complexation degree and in the carbene-NH_3 adduct density, along the membrane cross-section. The membrane actuator showed the highest sensitivity among the state-of-the-art soft proton actuators toward acetic acid at the 10^{-6} mol L^{-1} (M) level in aqueous media (Fig. 12d and e). Moreover, through the competing actuation of the two gradients, this material could monitor the progress of a proton-involved chemical reaction involving multiple stimuli and operational steps. This work constituted a significant step towards the real-life application of soft actuators in chemical sensing and reaction technology [111].

In addition, in response to the solvent vapor/liquid phase, porous PIL systems can be designed to respond to external chemical stimuli (*e.g.*, redox agents). For example, Vancso and coworkers [107] prepared poly (ferrocenylsilane) (PFS)-based PIL and PAA engineered redox-responsive porous PIL membranes *via* an electrostatic complexation method. The membranes showed switchable structures, between more- and less-porous states, accompanied by a color change from yellow (neutral state) to green (oxidized state) by varying the redox state of the ferrocenylsilane moieties in the membrane (Fig. 12f and g). This property was further exploited in redox-controlled gating, molecular separations and sensing applications.

4.4. Adsorption and separation

In the separation field, nanoporous PILs have been examined for the effective removal of heavy metal ions (*e.g.*, Cr(VI), Pb(II), and Hg(II)) and organic dyes (*e.g.*, methyl blue and methyl orange) because of their favorable electrostatic interactions [88]. Due to their highly polar pores, mesoporous PIL complexes are efficient absorbents for dye removal. Our group prepared mesoporous PIL complex membranes *via* the in situ ionic complexation of a PIL, poly(3-cyanomethyl-1-vinylimidazolium bis(trifluoromethanesulfonyl)imide), and multivalent carboxylic acids under

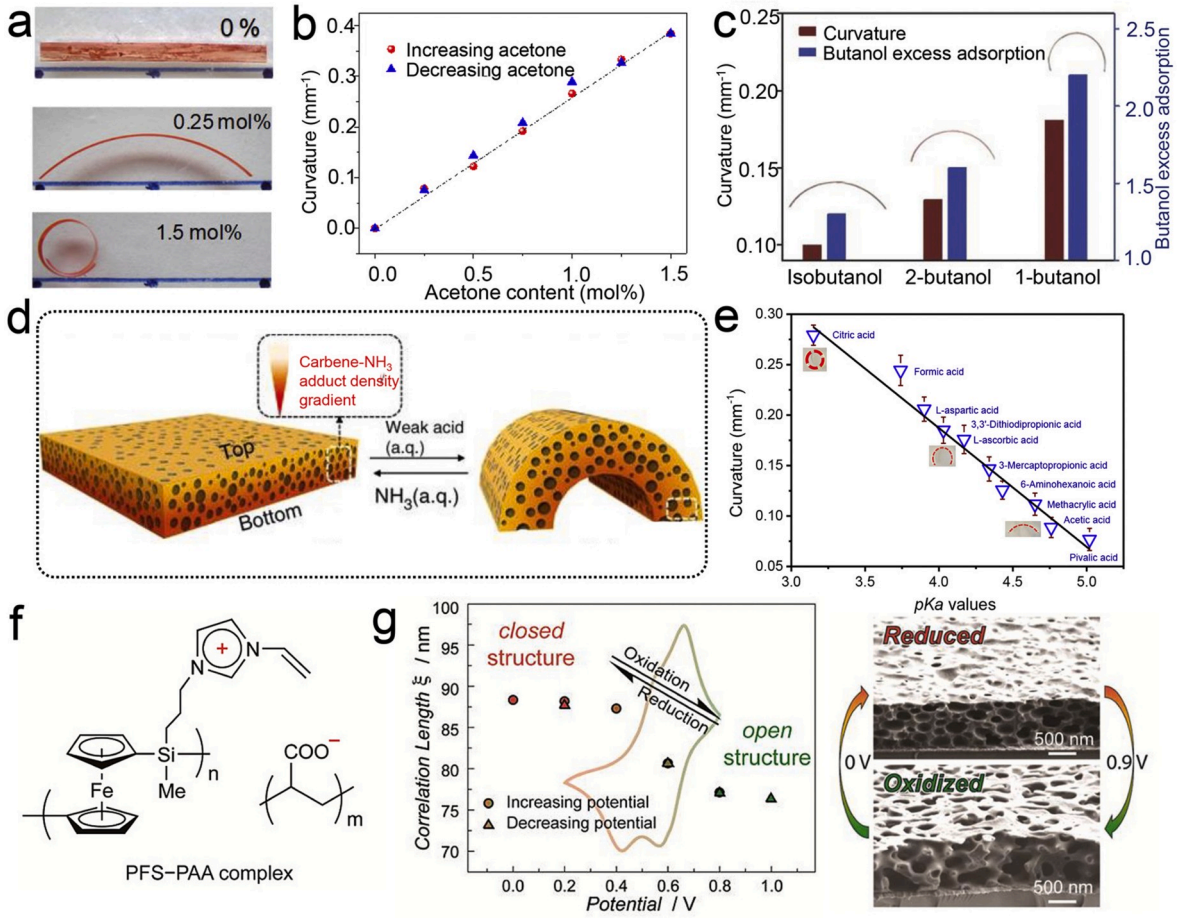

Fig. 12. (a) Shape deformation of the PIL-PAA membrane toward acetone-water mixtures with different acetone contents (mol%) at 20 °C. (b) Plot of the curvature (mm^{-1}) of the membrane actuator against acetone content (mol%); (c) the curvature (red column) and excess absorption of butanol isomers (blue column) by a PIL-PAA membrane actuator in water containing 1.25 mol% butanol isomers at 20 °C [49]. Copyright 2015, Wiley. (d) Schematic of the ptraiz-TA membrane bent in response to external weak acid and back to its initial state in weak base (a.q. NH_3). (e) The detection of weak acids with different pKa values by the ptraiz-TA membrane actuator [111]. Copyright 2018, Nature Publishing Group. (f) Chemical structure of porous membranes based on PFS and PAA. (g) Pore variations of reduced and oxidized porous membranes under different potentials [107]. Copyright 2017, American Chemical Society. (For interpretation of the references to color in this figure legend, the reader is referred to the Web version of this article.)

ammonia treatment [45,112]. A porous PIL complex with an S_{BET} of ~400 $m^2\ g^{-1}$ can absorb methyl orange from ethanol more efficiently than those of mesoporous silica or activated carbon because of the highly polarized ionic mesopores [112]. The functionalization of mesoporous PIL membranes with a photoresponsive azobenzene moiety can tune the porosity of the membrane upon UV irradiation, which provides as a platform for selective dye removal [113]. Instead of multivalent carboxylic acids with pillar[5]arene, Huang and coworkers prepared a meso/macroporous polymeric network *via* a similar electrostatic complexation between a positively charged PIL and a negatively charged carboxylated pillar[5]arene [114], and the resulting material had a high S_{BET} of up to 350 $m^2\ g^{-1}$. Such materials also show excellent performance in the separation of 1,6-hexanediol from $CDCl_3$, resulting from host–guest binding *via* C–H … π interactions between the carboxylated pillar[5]arene and 1,6-hexanediol.

5. Conclusions

Nanoporous PIL scaffolds can be readily constructed by template- or template-free methods, resulting in tailored macro-, meso-, or micropores, or a hierarchically porous structure. Template-assisted syntheses involve the polymerization of IL monomers in the presence of hard or soft templates and subsequent template removal, which can be complicated and is sometimes environmentally unfriendly. Building up porous complex PIL systems *via* in situ ionic complexation of a cationic PIL and polyacids/multiacids is comparably easy when a uniform pore size is not strictly required. In addition, postsynthetic modification serves as an alternative for converting neutral nanoporous polymers into nanoporous PILs.

Considering their excellent properties, including high thermal stability, wide electrochemical window, and reasonably high ionic conductivity, nanoporous PILs have been actively exploited as alternatives for IL electrolytes in batteries, as they can avoid the well-known IL leaching problem and act as separators to prevent short circuits between electrodes. Since the operation voltage strongly affects the energy density of electrochemical devices, it is highly desirable to search for nanoporous PIL-based electrolytes that can work at high voltage with sufficient electrochemical stability. Further studies should also focus on nanoporous PILs with engineered charge density and ion motion for enhanced Li^+ ion conduction or the development of nanoporous PILs with enhanced interfacial wettability toward electrodes by tuning the cations/anions.

Nanoporous PIL-derived heteroatom-doped porous carbon materials with adjustable morphologies are promising for energy and environmental applications. In particular, the development of carbon fibers and membranes possessing hierarchically nanoporous architectures opens up new directions for carbon-based membrane technologies. Further investigations of heteroatom-doped porous carbon materials, *i.e.*, S/B/P-

doped carbon or S/B/P–N codoped carbon, will greatly enrich their materials applications in energy-related fields.

In addition to the aforementioned applications, nanoporous PILs have emerged as novel functional materials in fields such as gas capture, catalysis, and sensing due to the synergy between the pores and the charged moieties. Recently, PILs have dramatically changed the research scope of traditional ionic polymers in terms of their interactions and compatibility with materials actively studied in related fields, such as inorganic materials, metal–organic hybrids and (bio)macromolecules [115,116]. Such attributes can greatly expand the applicability of PILs in combination with nanopores. In particular, the integration of functional sites in addition to intrinsic charges is promising for target-specific applications. For example, the polytriazolium PIL-derived polycarbene, which serves as a strong σ-donor and comparatively weak π-acceptor, can strongly bind to different substances ranging from metal/metal-organic complexes to *p*-block element-bearing compounds. The combination of micro-, meso-, and macropores with well-dispersed active sites may generate synergistic effects with enhanced performance for specific applications, *e.g.*, the integration of porous skeletons with tailored pore structures and polycarbene sites is promising for high-performance hydrogen generation catalysis [8], proton sensing [111], and CO_2 capture [95]. In this regard, intriguing functional site-decorated porous architectures and fantastic properties are expected and represent an exciting area with great opportunity for future advances.

Currently, the field of nanoporous PILs is still in its infancy. Due to their diverse structures of ionic monomers and the variety of synthetic methods available, there is much room to produce intriguing structures with fascinating physicochemical properties. In particular, the development of PILs with tunable chemical structures and controlled pore architectures as well as attractive properties such as superb ion conductivity, high porosity and large surface area for better mass transport will allow tailored solutions for the numerous problems in sustainable development. It will be exciting to witness the rapid development of this field, which is currently advancing applications in the fields of energy and the environment.

Declaration of competing interest

The authors declare that they have no known competing financial interests or personal relationships that could have appeared to influence the work reported in this paper.

CRediT authorship contribution statement

Huijuan Lin: Writing - original draft, Writing - original draft. **Suyun Zhang:** Writing - original draft, Writing - original draft. **Jian-Ke Sun:** Conceptualization, Writing - original draft, Conceptualization, Writing - original draft. **Markus Antonietti:** Writing - review & editing, Writing - review & editing. **Jiayin Yuan:** Writing - review & editing, Supervision, Writing - review & editing, Supervision.

Acknowledgements

This work was financially supported by start-up Grant form Beijing Institute of Technology (3100011181910). H. Lin thanks the financial support from the National Natural Science Foundation of China (51903121), the Natural Science Foundation of Jiangsu Higher Education Institutions (18KJB150016), the “Six Talent Peak” Project of Jiangsu Province (XCL-018), and Nanjing Tech University (start-up fund 3827400203 and 50235069). J. Yuan is grateful for financial support from European research council (ERC) Starting Grant NAPOLI-639720, Swedish Research Council Grant 2018-05351, Dozentenpreis 15126 from Verband der Chemischen Industrie e.V. (VCI) in Germany, the Wallenberg Academy Fellow program (Grant KAW 2017.0166) in Sweden, and the Stockholm University Strategic Fund SU FV-2.1.1-005.

References

[1] A.G. Slater, A.I. Cooper, Function-led design of new porous materials, Science 348 (2015) aaa8075.
[2] D. Wu, F. Xu, B. Sun, R. Fu, H. He, K. Matyjaszewski, Design and preparation of porous polymers, Chem. Rev. 112 (2012) 3959–4015.
[3] A. Thomas, Functional materials: from hard to soft porous frameworks, Angew. Chem. Int. Ed. 49 (2010) 8328–8344.
[4] D. Mukherjee, G. Gowda, Y.K.H. Makri Nimbegondi Kotresh, S. Sampath, Porous, hyper-cross-linked, three-dimensional polymer as stable, high rate capability electrode for lithium-ion battery, ACS Appl. Mater. Interfaces 9 (2017) 19446–19454.
[5] F. Wu, E. Zhao, D. Gordon, Y. Xiao, C. Hu, G. Yushin, Infiltrated porous polymer sheets as free-standing flexible lithium-sulfur battery electrodes, Adv. Mater. 28 (2016) 6365–6371.
[6] M.A. Shannon, P.W. Bohn, M. Elimelech, J.G. Georgiadis, B.J. Mariñas, A. M. Mayes, Science and technology for water purification in the coming decades, Nature 452 (2008) 301–310.
[7] N.V. Plechkova, K.R. Seddon, Applications of ionic liquids in the chemical industry, Chem. Soc. Rev. 37 (2008) 123–150.
[8] J.-K. Sun, Z. Kochovski, W.-Y. Zhang, H. Kirmse, Y. Lu, M. Antonietti, J. Yuan, General synthetic route toward highly dispersed metal clusters enabled by poly (ionic liquid)s, J. Am. Chem. Soc. 139 (2017) 8971–8976.
[9] S.-Y. Zhang, Z. Kochovski, H.-C. Lee, Y. Lu, H. Zhang, J. Zhang, J.-K. Sun, J. Yuan, Ionic organic cage-encapsulating phase-transferable metal clusters, Chem. Sci. 10 (2019) 1450–1456.
[10] J. von Zamory, M. Bedu, S. Fantini, S. Passerini, E. Paillard, Polymeric ionic liquid nanoparticles as binder for composite Li-ion electrodes, J. Power Sources 240 (2013) 745–752.
[11] S. Zulfiqar, M.I. Sarwar, D. Mecerreyes, Polymeric ionic liquids for CO_2 capture and separation: potential, progress and challenges, Polym. Chem. 6 (2015) 6435–6451.
[12] Y. Xie, Q. Sun, Y. Fu, L. Song, J. Liang, X. Xu, H. Wang, J. Li, S. Tu, X. Lu, J. Li, Sponge-like quaternary ammonium-based poly(ionic liquid)s for high CO_2 capture and efficient cycloaddition under mild conditions, J. Mater. Chem. A 5 (2017) 25594–25600.
[13] C. Willa, J. Yuan, M. Niederberger, D. Koziej, When nanoparticles meet poly(ionic liquid)s: chemoresistive CO_2 sensing at room temperature, Adv. Funct. Mater. 25 (2015) 2537–2542.
[14] P. Tamilarasan, S. Ramaprabhu, Integration of polymerized ionic liquid with graphene for enhanced CO_2 adsorption, J. Mater. Chem. A 3 (2015) 101–108.
[15] J.-P. Lindner, Imidazolium-based polymers via the poly-radziszewski reaction, Macromolecules 49 (2016) 2046–2053.
[16] K. Grygiel, Poly(ionic Liquid) Stabilizers and New Synthetic Approaches, Doctoral thesis, Universität Potsdam, 2015.
[17] J. Yuan, M. Antonietti, Poly(ionic liquid)s: polymers expanding classical property profiles, Polymer 52 (2011) 1469–1482.
[18] J. Yuan, D. Mecerreyes, M. Antonietti, Poly(ionic liquid)s: an update, Prog. Polym. Sci. 38 (2013) 1009–1036.
[19] W. Qian, J. Texter, F. Yan, Frontiers in poly(ionic liquid)s: syntheses and applications, Chem. Soc. Rev. 46 (2017) 1124–1159.
[20] S. Zhang, K. Dokko, M. Watanabe, Porous ionic liquids: synthesis and application, Chem. Sci. 6 (2015) 3684–3691.
[21] M. Ulbricht, Advanced functional polymer membranes, Polymer 47 (2006) 2217–2262.
[22] K.-V. Peinemann, V. Abetz, P.F.W. Simon, Asymmetric superstructure formed in a block copolymer via phase separation, Nat. Mater. 6 (2007) 992–996.
[23] P.D. Graham, A.J. Pervan, A.J. McHugh, The dynamics of thermal-induced phase separation in PMMA solutions, Macromolecules 30 (1997) 1651–1655.
[24] S. Jana, M. Anas, T. Maji, S. Banerjee, T.K. Mandal, Tryptophan-based styryl homopolymer and polyzwitterions with solvent-induced UCST, ion-induced LCST and pH-induced UCST, Polym. Chem. 10 (2019) 526–538.
[25] W. Zhang, Q. Zhao, J. Yuan, Porous polyelectrolytes: the interplay of charge and pores for new functionalities, Angew. Chem. Int. Ed. 57 (2018) 6754–6773.
[26] D. Mecerreyes, Polymeric ionic liquids: broadening the properties and applications of polyelectrolytes, Prog. Polym. Sci. 36 (2011) 1629–1648.
[27] J.-K. Sun, M. Antonietti, J. Yuan, Nanoporous ionic organic networks: from synthesis to materials applications, Chem. Soc. Rev. 45 (2016) 6627–6656.
[28] K.R. Phillips, G.T. England, S. Sunny, E. Shirman, T. Shirman, N. Vogel, J. Aizenberg, A colloidoscope of colloid-based porous materials and their uses, Chem. Soc. Rev. 45 (2016) 281–322.
[29] J. Huang, C.-a. Tao, Q. An, C. Lin, X. Li, D. Xu, Y. Wu, X. Li, D. Shen, G. Li, Visual indication of enviromental humidity by using poly(ionic liquid) photonic crystals, Chem. Commun. 46 (2010) 4103–4105.
[30] X. Hu, J. Huang, W. Zhang, M. Li, C. Tao, G. Li, Photonic ionic liquids polymer for naked-eye detection of anions, Adv. Mater. 20 (2008) 4074–4078.
[31] J. Huang, C.-a. Tao, Q. An, W. Zhang, Y. Wu, X. Li, D. Shen, G. Li, 3D-ordered macroporous poly(ionic liquid) films as multifunctional materials, Chem. Commun. 46 (2010) 967–969.
[32] J. Cui, W. Zhu, N. Gao, J. Li, H. Yang, Y. Jiang, P. Seidel, B.J. Ravoo, G. Li, Inverse opal spheres based on polyionic liquids as functional microspheres with tunable optical properties and molecular recognition capabilities, Angew. Chem. Int. Ed. 53 (2014) 3844–3848.
[33] A. Wilke, J. Yuan, M. Antonietti, J. Weber, Enhanced carbon dioxide adsorption by a mesoporous poly(ionic liquid), ACS Macro Lett. 1 (2012) 1028–1031.

[34] P. Zhang, Z.-A. Qiao, X. Jiang, G.M. Veith, S. Dai, Nanoporous ionic organic networks: stabilizing and supporting gold nanoparticles for catalysis, Nano Lett. 15 (2015) 823–828.

[35] H. Zhu, Z. Liu, Y. Wang, D. Kong, X. Yuan, Z. Xie, Nanosized $CaCO_3$ as hard template for creation of intracrystal pores within silicalite-1 crystal, Chem. Mater. 20 (2008) 1134–1139.

[36] H. Liu, C.-Y. Cao, F.-F. Wei, Y. Jiang, Y.-B. Sun, P.-P. Huang, W.-G. Song, Fabrication of macroporous/mesoporous carbon nanofiber using $CaCO_3$ nanoparticles as dual purpose template and its application as catalyst support, J. Phys. Chem. C 117 (2013) 21426–21432.

[37] D. Kowalski, A. Tighineanu, P. Schmuki, Polymer nanowires or nanopores? Site selective filling of titania nanotubes with polypyrrole, J. Mater. Chem. 21 (2011) 17909–17915.

[38] S. Shukla, K.-T. Kim, A. Baev, Y.K. Yoon, N.M. Litchinitser, P.N. Prasad, Fabrication and characterization of gold−polymer nanocomposite plasmonic nanoarrays in a porous alumina template, ACS Nano 4 (2010) 2249–2255.

[39] G.J.d.A.A. Soler-Illia, C. Sanchez, B. Lebeau, J. Patarin, Chemical strategies to design textured materials: from microporous and mesoporous oxides to nanonetworks and hierarchical structures, Chem. Rev. 102 (2002) 4093–4138.

[40] C. Gao, G. Chen, X. Wang, J. Li, Y. Zhou, J. Wang, A hierarchical meso-macroporous poly(ionic liquid) monolith derived from a single soft template, Chem. Commun. 51 (2015) 4969–4972.

[41] I. Azcune, I. García, P.M. Carrasco, A. Genua, M. Tanczyk, M. Jaschik, K. Warmuzinski, G. Cabañero, I. Odriozola, Facile and scalable synthesis of nanoporous materials based on poly(ionic liquid)s, ChemSusChem 7 (2014) 3407–3412.

[42] X. Suo, L. Xia, Q. Yang, Z. Zhang, Z. Bao, Q. Ren, Y. Yang, H. Xing, Synthesis of anion-functionalized mesoporous poly(ionic liquid)s via a microphase separation-hypercrosslinking strategy: highly efficient adsorbents for bioactive molecules, J. Mater. Chem. A 5 (2017) 14114–14123.

[43] X. Feng, C. Gao, Z. Guo, Y. Zhou, J. Wang, Pore structure controllable synthesis of mesoporous poly(ionic liquid)s by copolymerization of alkylvinylimidazolium salts and divinylbenzene, RSC Adv. 4 (2014) 23389–23395.

[44] X. Wang, J. Li, G. Chen, Z. Guo, Y. Zhou, J. Wang, Hydrophobic mesoporous poly (ionic liquid)s towards highly efficient and contamination-resistant solid-base catalysts, ChemCatChem 7 (2015) 993–1003.

[45] Q. Zhao, P. Zhang, M. Antonietti, J. Yuan, Poly(ionic liquid) complex with spontaneous micro-/mesoporosity: template-free synthesis and application as catalyst support, J. Am. Chem. Soc. 134 (2012) 11852–11855.

[46] Q. Zhao, M. Yin, A.P. Zhang, S. Prescher, M. Antonietti, J. Yuan, Hierarchically structured nanoporous poly(ionic liquid) membranes: facile preparation and application in fiber-optic pH sensing, J. Am. Chem. Soc. 135 (2013) 5549–5552.

[47] K. Täuber, Q. Zhao, M. Antonietti, J. Yuan, Tuning the pore size in gradient poly (ionic liquid) membranes by small organic acids, ACS Macro Lett. 4 (2015) 39–42.

[48] K. Täuber, A. Zimathies, J. Yuan, Porous membranes built up from hydrophilic poly(ionic liquid)s, Macromol. Rapid Commun. 36 (2015) 2176–2180.

[49] Q. Zhao, J. Heyda, J. Dzubiella, K. Täuber, J.W.C. Dunlop, J. Yuan, Sensing solvents with ultrasensitive porous poly(ionic liquid) actuators, Adv. Mater. 27 (2015) 2913–2917.

[50] M.-J. Yin, Q. Zhao, J. Wu, K. Seefeldt, J. Yuan, Precise micropatterning of a porous poly(ionic liquid) via maskless photolithography for high-performance nonenzymatic H_2O_2 sensing, ACS Nano 12 (2018) 12551–12557.

[51] K. Täuber, A. Dani, J. Yuan, Covalent cross-linking of porous poly(ionic liquid) membrane via a triazine network, ACS Macro Lett. 6 (2017) 1–5.

[52] F. Liu, L. Wang, Q. Sun, L. Zhu, X. Meng, F.-S. Xiao, Transesterification catalyzed by ionic liquids on superhydrophobic mesoporous polymers: heterogeneous catalysts that are faster than homogeneous catalysts, J. Am. Chem. Soc. 134 (2012) 16948–16950.

[53] R. Xing, N. Liu, Y. Liu, H. Wu, Y. Jiang, L. Chen, M. He, P. Wu, Novel solid acid catalysts: sulfonic acid group-functionalized mesostructured polymers, Adv. Funct. Mater. 17 (2007) 2455–2461.

[54] L. Qin, B. Wang, Y. Zhang, L. Chen, G. Gao, Anion exchange: a novel way of preparing hierarchical porous structure in poly(ionic liquid)s, Chem. Commun. 53 (2017) 3785–3788.

[55] F. Yan, J. Texter, Solvent-reversible poration in ionic liquid copolymers, Angew. Chem. Int. Ed. 46 (2007) 2440–2443.

[56] F. Yan, J. Texter, Surfactant ionic liquid-based microemulsions for polymerization, Chem. Commun. (2006) 2696–2698.

[57] P. Schaaf, J.B. Schlenoff, Saloplastics: processing compact polyelectrolyte complexes, Adv. Mater. 27 (2015) 2420–2432.

[58] H.H. Hariri, J.B. Schlenoff, Saloplastic macroporous polyelectrolyte complexes: cartilage mimics, Macromolecules 43 (2010) 8656–8663.

[59] M. Li, L. Yang, S. Fang, S. Dong, S.-i. Hirano, K. Tachibana, Polymerized ionic liquids with guanidinium cations as host for gel polymer electrolytes in lithium metal batteries, Polym. Int. 61 (2012) 259–264.

[60] M. Li, B. Yang, L. Wang, Y. Zhang, Z. Zhang, S. Fang, Z. Zhang, New polymerized ionic liquid (PIL) gel electrolyte membranes based on tetraalkylammonium cations for lithium ion batteries, J. Membr. Sci. 447 (2013) 222–227.

[61] J.H. Lee, J.S. Lee, J.-W. Lee, S.M. Hong, C.M. Koo, Ion transport behavior in polymerized imidazolium ionic liquids incorporating flexible pendant groups, Eur. Polym. J. 49 (2013) 1017–1022.

[62] G.B. Appetecchi, G.T. Kim, M. Montanina, M. Carewska, R. Marcilla, D. Mecerreyes, I. De Meatza, Ternary polymer electrolytes containing pyrrolidinium-based polymeric ionic liquids for lithium batteries, J. Power Sources 195 (2010) 3668–3675.

[63] M. Li, L. Wang, B. Yang, T. Du, Y. Zhang, Facile preparation of polymer electrolytes based on the polymerized ionic liquid poly((4-vinylbenzyl) trimethylammonium bis(trifluoromethanesulfonylimide)) for lithium secondary batteries, Electrochim. Acta 123 (2014) 296–302.

[64] K. Yin, Z. Zhang, L. Yang, S.-I. Hirano, An imidazolium-based polymerized ionic liquid via novel synthetic strategy as polymer electrolytes for lithium ion batteries, J. Power Sources 258 (2014) 150–154.

[65] K. Yin, Z. Zhang, X. Li, L. Yang, K. Tachibana, S.-i. Hirano, Polymer electrolytes based on dicationic polymeric ionic liquids: application in lithium metal batteries, J. Mater. Chem. A 3 (2015) 170–178.

[66] D. Zhou, R. Liu, J. Zhang, X. Qi, Y.-B. He, B. Li, Q.-H. Yang, Y.-S. Hu, F. Kang, In situ synthesis of hierarchical poly(ionic liquid)-based solid electrolytes for high-safety lithium-ion and sodium-ion batteries, Nano Energy 33 (2017) 45–54.

[67] J. Fang, H. Xu, X. Wei, M. Guo, X. Lu, C. Lan, Y. Zhang, Y. Liu, T. Peng, Preparation and characterization of quaternized poly(2,2,2-trifluoroethyl methacrylate-co-N-vinylimidazole) membrane for vanadium redox flow battery, Polym. Adv. Technol. 24 (2013) 168–173.

[68] D. Chen, M.A. Hickner, E. Agar, E.C. Kumbur, Optimized anion exchange membranes for vanadium redox flow batteries, ACS Appl. Mater. Interfaces 5 (2013) 7559–7566.

[69] W. Lu, Z. Yuan, M. Li, X. Li, H. Zhang, I. Vankelecom, Solvent-induced rearrangement of ion-transport channels: a way to create advanced porous membranes for vanadium flow batteries, Adv. Funct. Mater. 27 (2017) 1604587.

[70] X. Yan, C. Zhang, Z. Dong, B. Jiang, Y. Dai, X. Wu, G. He, Amphiprotic side-chain functionalization constructing highly proton/vanadium-selective transport channels for high-performance membranes in vanadium redox flow batteries, ACS Appl. Mater. Interfaces 10 (2018) 32247–32255.

[71] Z. Yuan, Y. Duan, H. Zhang, X. Li, H. Zhang, I. Vankelecom, Advanced porous membranes with ultra-high selectivity and stability for vanadium flow batteries, Energy Environ. Sci. 9 (2016) 441–447.

[72] T.N.L. Doan, T.K.A. Hoang, P. Chen, Recent development of polymer membranes as separators for all-vanadium redox flow batteries, RSC Adv. 5 (2015) 72805–72815.

[73] X. Li, H. Zhang, Z. Mai, H. Zhang, I. Vankelecom, Ion exchange membranes for vanadium redox flow battery (VRB) applications, Energy Environ. Sci. 4 (2011) 1147–1160.

[74] Y. Xing, L. Liu, C. Wang, N. Li, Side-chain-type anion exchange membranes for vanadium flow battery: properties and degradation mechanism, J. Mater. Chem. A 6 (2018) 22778–22789.

[75] H. Zhang, H. Zhang, F. Zhang, X. Li, Y. Li, I. Vankelecom, Advanced charged membranes with highly symmetric spongy structures for vanadium flow battery application, Energy Environ. Sci. 6 (2013) 776–781.

[76] Y. Zhao, M. Li, Z. Yuan, X. Li, H. Zhang, I.F.J. Vankelecom, Advanced charged sponge-like membrane with ultrahigh stability and selectivity for vanadium flow batteries, Adv. Funct. Mater. 26 (2016) 210–218.

[77] J. Yuan, C. Giordano, M. Antonietti, Ionic liquid monomers and polymers as precursors of highly conductive, mesoporous, graphitic carbon nanostructures, Chem. Mater. 22 (2010) 5003–5012.

[78] J. Yuan, H. Schlaad, C. Giordano, M. Antonietti, Double hydrophilic diblock copolymers containing a poly(ionic liquid) segment: controlled synthesis, solution property, and application as carbon precursor, Eur. Polym. J. 47 (2011) 772–781.

[79] Q. Qin, Y. Liu, W. Shan, W. Hou, K. Wang, X. Ling, Y. Zhou, J. Wang, Synergistic catalysis of Fe_2O_3 nanoparticles on mesoporous poly(ionic liquid)-derived carbon for benzene hydroxylation with dioxygen, Ind. Eng. Chem. Res. 56 (2017) 12289–12296.

[80] X. Wang, S. Dai, Ionic liquids as versatile precursors for functionalized porous carbon and carbon–oxide composite materials by confined carbonization, Angew. Chem. Int. Ed. 49 (2010) 6664–6668.

[81] J.S. Lee, X. Wang, H. Luo, S. Dai, Fluidic carbon precursors for formation of functional carbon under ambient pressure based on ionic liquids, Adv. Mater. 22 (2010) 1004–1007.

[82] P.F. Fulvio, P.C. Hillesheim, Y. Oyola, S.M. Mahurin, G.M. Veith, S. Dai, A new family of fluidic precursors for the self-templated synthesis of hierarchical nanoporous carbons, Chem. Commun. 49 (2013) 7289–7291.

[83] J.S. Lee, X. Wang, H. Luo, G.A. Baker, S. Dai, Facile ionothermal synthesis of microporous and mesoporous carbons from task specific ionic liquids, J. Am. Chem. Soc. 131 (2009) 4596–4597.

[84] H. Wang, S. Min, C. Ma, Z. Liu, W. Zhang, Q. Wang, D. Li, Y. Li, S. Turner, Y. Han, H. Zhu, E. Abou-hamad, M.N. Hedhili, J. Pan, W. Yu, K.-W. Huang, L.-J. Li, J. Yuan, M. Antonietti, T. Wu, Synthesis of single-crystal-like nanoporous carbon membranes and their application in overall water splitting, Nat. Commun. 8 (2017) 13592.

[85] J. Yuan, A.G. Márquez, J. Reinacher, C. Giordano, J. Janek, M. Antonietti, Nitrogen-doped carbon fibers and membranes by carbonization of electrospun poly(ionic liquid)s, Polym. Chem. 2 (2011) 1654–1657.

[86] H. Wang, J. Jia, P. Song, Q. Wang, D. Li, S. Min, C. Qian, L. Wang, Y.F. Li, C. Ma, T. Wu, J. Yuan, M. Antonietti, G.A. Ozin, Efficient electrocatalytic reduction of CO_2 by nitrogen-doped nanoporous carbon/carbon nanotube membranes: a step towards the electrochemical CO_2 refinery, Angew. Chem. Int. Ed. 56 (2017) 7847–7852.

[87] H. Wang, S. Min, Q. Wang, D. Li, G. Casillas, C. Ma, Y. Li, Z. Liu, L.-J. Li, J. Yuan, M. Antonietti, T. Wu, Nitrogen-doped nanoporous carbon membranes with Co/CoP janus-type nanocrystals as hydrogen evolution electrode in both acidic and alkaline environments, ACS Nano 11 (2017) 4358–4364.

[88] Y. Ren, J. Zhang, J. Guo, F. Chen, F. Yan, Porous poly(ionic liquid) membranes as efficient and recyclable absorbents for heavy metal ions, Macromol. Rapid Commun. 38 (2017) 1700151.
[89] H. Mi, Z. Jiang, J. Kong, Hydrophobic poly(ionic liquid) for highly effective separation of methyl blue and chromium ions from water, Polymers 5 (2013) 1203–1214.
[90] J. Tang, H. Tang, W. Sun, M. Radosz, Y. Shen, Low-pressure CO_2 sorption in ammonium-based poly(ionic liquid)s, Polymer 46 (2005) 12460–12467.
[91] J. Tang, W. Sun, H. Tang, M. Radosz, Y. Shen, Enhanced CO_2 absorption of poly (ionic liquid)s, Macromolecules 38 (2005) 2037–2039.
[92] J. Tang, Y. Shen, M. Radosz, W. Sun, Isothermal carbon dioxide sorption in poly (ionic liquid)s, Ind. Eng. Chem. Res. 48 (2009) 9113–9118.
[93] H. Zhou, W.-Z. Zhang, Y.-M. Wang, J.-P. Qu, X.-B. Lu, N-heterocyclic carbene functionalized polymer for reversible fixation−release of CO_2, Macromolecules 42 (2009) 5419–5421.
[94] J. Pinaud, J. Vignolle, Y. Gnanou, D. Taton, Poly(N-heterocyclic-carbene)s and their CO_2 adducts as recyclable polymer-supported organocatalysts for benzoin condensation and transesterification reactions, Macromolecules 44 (2011) 1900–1908.
[95] S. Soll, Q. Zhao, J. Weber, J. Yuan, Activated CO_2 sorption in mesoporous imidazolium-type poly(ionic liquid)-based polyampholytes, Chem. Mater. 25 (2013) 3003–3010.
[96] Q. Wang, X. Ling, T. Ye, Y. Zhou, J. Wang, Ionic mesoporous polyamides enable highly dispersed ultrafine Ru nanoparticles: a synergistic stabilization effect and remarkable efficiency in levulinic acid conversion into γ-valerolactone, J. Mater. Chem. A 7 (2019) 19140–19151.
[97] Q. Wang, X. Cai, Y. Liu, J. Xie, Y. Zhou, J. Wang, Pd nanoparticles encapsulated into mesoporous ionic copolymer: efficient and recyclable catalyst for the oxidation of benzyl alcohol with O_2 balloon in water, Appl. Catal. B Environ. 189 (2016) 242–251.
[98] W. Hou, Q. Wang, Z. Guo, J. Li, Y. Zhou, J. Wang, Nanobelt α-CuV_2O_6 with hydrophilic mesoporous poly(ionic liquid): a binary catalyst for synthesis of 2,5-diformylfuran from fructose, Catal. Sci. Technol. 7 (2017) 1006–1016.
[99] X. Wang, Y. Zhou, Z. Guo, G. Chen, J. Li, Y. Shi, Y. Liu, J. Wang, Heterogeneous conversion of CO_2 into cyclic carbonates at ambient pressure catalyzed by ionothermal-derived meso-macroporous hierarchical poly(ionic liquid)s, Chem. Sci. 6 (2015) 6916–6924.
[100] Z. Guo, X. Cai, J. Xie, X. Wang, Y. Zhou, J. Wang, Hydroxyl-exchanged nanoporous ionic copolymer toward low-temperature cycloaddition of atmospheric carbon dioxide into carbonates, ACS Appl. Mater. Interfaces 8 (2016) 12812–12821.
[101] Y. Xie, J. Liang, Y. Fu, M. Huang, X. Xu, H. Wang, S. Tu, J. Li, Hypercrosslinked mesoporous poly(ionic liquid)s with high ionic density for efficient CO_2 capture and conversion into cyclic carbonates, J. Mater. Chem. A 6 (2018) 6660–6666.
[102] J. Cao, W. Shan, Q. Wang, X. Ling, G. Li, Y. Lyu, Y. Zhou, J. Wang, Ordered porous poly(ionic liquid) crystallines: spacing confined ionic surface enhancing selective CO_2 capture and fixation, ACS Appl. Mater. Interfaces 11 (2019) 6031–6041.
[103] K. Täuber, B. Lepenies, J. Yuan, Polyvinylpyridinium-type gradient porous membranes: synthesis, actuation and intrinsic cell growth inhibition, Polym. Chem. 6 (2015) 4855–4858.
[104] J.-K. Sun, H.-J. Lin, W.-Y. Zhang, M.-R. Gao, M. Antonietti, J. Yuan, A tale of two membranes: from poly (ionic liquid) to metal–organic framework hybrid nanoporous membranes via pseudomorphic replacement, Mater. Horiz. 4 (2017) 681–687.
[105] J.-K. Sun, Y.-J. Zhang, G.-P. Yu, J. Zhang, M. Antonietti, J. Yuan, Three birds, one stone – photo-/piezo-/chemochromism in one conjugated nanoporous ionic organic network, J. Mater. Chem. C 6 (2018) 9065–9070.
[106] F. Chen, Y. Ren, J. Guo, F. Yan, Thermo- and electro-dual responsive poly(ionic liquid) electrolyte based smart windows, Chem. Commun. 53 (2017) 1595–1598.
[107] L. Folkertsma, K. Zhang, O. Czakkel, H.L. de Boer, M.A. Hempenius, A. van den Berg, M. Odijk, G.J. Vancso, Synchrotron SAXS and impedance spectroscopy unveil nanostructure variations in redox-responsive porous membranes from poly (ferrocenylsilane) poly(ionic liquid)s, Macromolecules 50 (2017) 296–302.
[108] B. Wu, W. Zhang, N. Gao, M. Zhou, Y. Liang, Y. Wang, F. Li, G. Li, Poly (ionic liquid)-based breath figure films: a new kind of honeycomb porous films with great extendable capability, Sci. Rep. 7 (2017) 13973.
[109] W. Zhang, Y. Li, Y. Liang, N. Gao, C. Liu, S. Wang, X. Yin, G. Li, Poly(ionic liquid)s as a distinct receptor material to create a highly-integrated sensing platform for efficiently identifying numerous saccharides, Chem. Sci. 10 (2019) 6617–6623.
[110] Q. Zhao, J.W.C. Dunlop, X. Qiu, F. Huang, Z. Zhang, J. Heyda, J. Dzubiella, M. Antonietti, J. Yuan, An instant multi-responsive porous polymer actuator driven by solvent molecule sorption, Nat. Commun. 5 (2014) 4293.
[111] J.-K. Sun, W. Zhang, R. Guterman, H.-J. Lin, J. Yuan, Porous polycarbene-bearing membrane actuator for ultrasensitive weak-acid detection and real-time chemical reaction monitoring, Nat. Commun. 9 (2018) 1717.
[112] Q. Zhao, S. Soll, M. Antonietti, J. Yuan, Organic acids can crosslink poly(ionic liquid)s into mesoporous polyelectrolyte complexes, Polym. Chem. 4 (2013) 2432–2435.
[113] A. Wu, F. Lu, M. Zhao, N. Sun, L. Shi, L. Zheng, Photo and humidity responsive mesoporous poly(ionic liquid) membrane for selective dye adsorption, ChemistrySelect 2 (2017) 1878–1884.
[114] Z. Zhang, Q. Zhao, J. Yuan, M. Antonietti, F. Huang, A hybrid porous material from a pillar[5]arene and a poly(ionic liquid): selective adsorption of n-alkylene diols, Chem. Commun. 50 (2014) 2595–2597.
[115] S.-Y. Zhang, Q. Zhuang, M. Zhang, H. Wang, Z. Gao, J.-K. Sun, J. Yuan, Poly(ionic liquid) composites, Chem. Soc. Rev. 49 (2020) 1726–1755.
[116] J.-K. Sun, Y.I. Sobolev, W. Zhang, Q. Zhuang, B.A. Grzybowski, Enhancing crystal growth using polyelectrolyte solutions and shear flow, Nature 579 (2020) 73–79.